

For Reference

NOT TO BE TAKEN FROM THIS ROOM

EX LIBRIS
UNIVERSITATIS
ALBERTAENSIS



THE UNIVERSITY OF ALBERTA

RELEASE FORM

NAME OF AUTHOR Brian C. Flintoff.....
TITLE OF THESIS The Cataphoretic Clarification.....
..... of Colloidal Suspensions in a
..... Continuous Thickener
DEGREE FOR WHICH THESIS WAS PRESENTED Master of Science
YEAR THIS DEGREE GRANTED 1975

Permission is hereby granted to THE UNIVERSITY OF ALBERTA LIBRARY to reproduce single copies of this thesis and to lend or sell such copies for private, scholarly or scientific research purposes only.

The author reserves other publication rights, and neither the thesis nor extensive extracts from it may be printed or otherwise reproduced without the author's written permission.

THE UNIVERSITY OF ALBERTA

THE CATAPHORETIC CLARIFICATION OF COLLOIDAL SUSPENSIONS
IN A CONTINUOUS THICKENER

by



BRIAN C. FLINTOFF

A THESIS

SUBMITTED TO THE FACULTY OF GRADUATE STUDIES AND RESEARCH
IN PARTIAL FULFILMENT OF THE REQUIREMENTS FOR THE DEGREE
OF MASTER OF SCIENCE

DEPARTMENT MINERAL ENGINEERING

EDMONTON, ALBERTA

SPRING, 1975

THE UNIVERSITY OF ALBERTA
FACULTY OF GRADUATE STUDIES AND RESEARCH

The undersigned certify that they have read, and
recommend to the Faculty of Graduate Studies and Research, for
acceptance, a thesis entitled The Cataphoretic Clarification
of Colloidal Suspensions in a Continuous Thickener.....
.....
submitted by Brian C. Flintoff.....
in partial fulfilment of the requirements for the degree of
Master of Science.....

To Marilyn

ABSTRACT

The principle of using cataphoresis to assist gravitational sedimentation of colloidal suspensions in a continuous thickener has been investigated. The results of preliminary tests indicated that minus 400 mesh silica flour would be the best material to use in forming suspensions for the elucidation of the operating characteristics of such a system. The operating characteristics which give the best clarification under the test conditions include; a) maximum voltage gradient at minimum power, and b) minimum solids feed rate combined with minimum overflow flowrate, and, c) controlled ionic strength in the suspension, and finally, d) a sufficiently large separation between the upper electrode and the feed well discharge. Under these conditions for silica, excellent clarification was achieved. Experiments were carried out on a bentonite suspension, and, a clay suspension created from a sample taken at the Great Canadian Oil Sands plant at Fort MacMurray, in Northeastern Alberta. The results from these tests show that some degree of clarification can be achieved but under present operating conditions this type of application appears to be economically impractical for these suspensions.

ACKNOWLEDGEMENTS

The author would like to express his sincere appreciation to all those people who assisted during the course of this work. In particular thanks is due to Professor L. R. Plitt who provided the research topic together with very valuable assistance in this project.

The author would also like to acknowledge the invaluable help provided by the departmental technical staff; B. Snider, T. Forman, E. Soetart, R. Scott, B. Konzuk and G. Chiasson.

Additional thanks are due to the people responsible for the typing of this script, Ms. P. Archibald and Ms. G. Malcolm.

The author wishes to thank the Chevron Oil Company of Canada for their financial sponsorship of this project.

TABLE OF CONTENTS

	PAGE
INTRODUCTION.....	1
PREVIOUS APPLICATIONS OF CATAPHORESIS.....	4
THEORETICAL REVIEW	
A The Origin of the Charge at the Mineral Water Interface.....	7
B Electrical Double Layer Theory.....	10
C Principles of Cataphoresis.....	24
D Basic Thickener Theory.....	27
EXPERIMENTAL	
A Materials.....	32
B Experimental Apparatus.....	33
C Experimental Procedure.....	37
EXPERIMENTAL RESULTS AND DISCUSSION	
A Batch Tests	42
B Elucidation of Operating Characteristics of the Continuous Thickener with Cataphoretic Assistance.....	44
C Bentonite Tests.....	95
D Great Canadian Oil Sands Test.....	101
CONCLUSIONS.....	106

REFERENCES.....	110
APPENDIX 1	113
APPENDIX 2	120

LIST OF TABLES

Table	Description	Page
1	Characteristics of Silica and Bentonite	32
2	Suspension Characteristics for Batch Testing	42
3	Edmonton City Water Analysis	47
4	Conditions for Test Number 1	54
5	Solutions to Stokes' Equation for Sample Calculation	62
6	Conditions for Test Number 2	64
7	Regression of Equation 8 for Overflow Clarity vs Applied Voltage or Power	69
8	Conditions for Test Number 3	73
9	Salt Concentration Buildup as a Function of Season	78
10	Conditions for Test Number 4	81
11	Conditions for Test Number 5	86
12	Conditions for Test Number 6	91
13	Conditions for Bentonite Test Number 2	96
14	Great Canadian Oil Sands Test Data	103
15	Comparative Economics and Efficiencies for Suspensions Treated	108

LIST OF FIGURES

Figures		Page
1	Schematic Illustration of the Electric Double Layer	12
2	The Variation of Potential with Distance from the Particle Surface When There are Potential Determining Ions Distinct from the Surface	13
3	The Effect of Different Electrolytes on the Zeta Potential of a Silica Colloid	19
4	The Zones Occurring in a Continuous Thickener Operated Within Capacity	30
5	Cataphoretic Mobility of -400 Mesh Silica Flour Versus pH of a Silica-Tap Water Suspension	46
6	Size Analysis of -400 Mesh Silica Flour as Determined by Both Cyclosizer and Hydrometer Techniques	51
7	The Density of Water as a Function of Temperature	53
8	Temperature Profiles for Test 1	55
9	Underflow Solids Concentration Versus Time for Test 1	57
10	Overflow Clarity Versus Time for Test 1	58
11	Overflow Clarity Versus Time for Test 2	65
12	Overflow Clarity as a Function of Applied Voltage for Test 2	66
13	Overflow Clarity as a Function of Power Input for Test 2	67
14	Overflow Clarity as a Function of Volumetric Overflow Flowrate for Test 3	74
15	Silica Particle Mobility as a Function of Sodium (from Sodium Chloride) Concentration	80
16	Overflow Clarity as a Function of Power and Voltage with Sodium Chloride Additions, for Test 4	82
17	Overflow Clarity as a Function of Both Voltage Gradient and Electrode Separation, for Test 5	87

List of Figures (cont'd)

Figures		Page
18	Overflow Clarity as a Function of Solids Feedrate Both With and Without Cataphoretic Assistance, for Test 6	92
19	Overflow Clarity Versus Time for the Bentonite Test 2	98
20	An Illustration of the Effectiveness of the Experimental Apparatus in Treating Bentonite and Silica Suspensions	99
21	Overflow Clarity Versus Time for the Great Canadian Oil Sands Test	104
22	Schematic of the Cataphoretically Assisted Thickener Clarifier Apparatus	114
23	Schematic Illustration of Mobility Measurement Apparatus	119

LIST OF PHOTOGRAPHIC PLATES

Plate	Description	Page
1	The Slurry Reservoir Tank and Refrigeration Equipment	115
2	The Slurry Feed System	116
3	The Thickener and Power Source	117
4	The Underflow and Slurry Return Pumps	118

INTRODUCTION

In recent years, clarification of solid-liquid suspensions has gained importance in industrial processing. Society has become very aware of environmental problems and is demanding more stringent controls on the quality of effluent from such processes. Governments are legislating new laws concerning the content of process discharge or waste and they are much more restrictive than in the past. As a consequence, industry finds itself faced with additional expense to meet the required standards and in some cases complex technological problems are encountered in the attempt to obey these laws. In addition to being an ecological problem, clarification is very important in the actual processing. For example, with the present system of recycling water in the industrial operations to minimize both fresh water usage and waste impoundment area and possibly reduce reagent consumption, the water must meet certain standards such that no deleterious effects on process efficiency are experienced. The clarity of the water used in processing and discharged from the process is very much an important factor in industrial design and operation.

The solid-liquid pulps which are the most difficult to clarify are those which contain particles which exhibit colloidal behaviour. A general definition which is used to classify suspensions defines those particles which have

a diameter of less than one micron to be in colloidal suspension, and, those particles having a diameter greater than this value to be in coarse suspension. In mineral processing both types of suspensions are encountered. For the purposes of this work, suspended solids which for practical purposes do not settle under the influence of gravity, will be referred to as being colloidal in nature.

In mineral processing, three different forces can be used for clarification. When it is desirable to remove the solid from the liquid both gravitational and centrifugal forces may be employed. In removing the liquid from the solid, a pressure gradient is used. Thickeners and settling ponds rely on gravitational force to cause sedimentation producing a product at the bottom which has a higher solids concentration than the feed and ideally, a clear water supernatant. Centrifuges and cyclones utilize centrifugal force to deposit the solids and the products are similar to the above. Filters employ either an applied pressure or vacuum to produce these products. When centrifugal force or pressure gradients are used in clarifying there is a relatively high cost per unit clarified since energy must be put into the system. On the other hand, thickeners and settling ponds use a natural force and thus provide an inexpensive means of clarification. The thickener, because of its simple operating characteristics, size, and low cost per unit clarified, was chosen for use in this project.

There are other, less widely used techniques for

clarification, such as, freezing out the solids, x-ray bombardment, spherical agglomeration, high intensity magnetic separation, applications of cataphoresis and flocculation. The latter is frequently used as an aid to increase the efficiency of both filters and thickeners. If the dosage is low enough to be economical and give good clarity flocculation is probably the best means of ensuring a clear discharge. In some cases flocculation cannot meet these requirements and as a consequence other techniques must be investigated. Cataphoresis is thought to be the best alternative, where it can be applied, since it makes use of the naturally formed surface charge on a particle and it is quite dependable. Filters have been constructed which make use of this cataphoretic technique and some are in use today in large scale industrial operations. The technique has never been applied to thickening although the idea that cataphoresis be used in conjunction with gravitational sedimentation has frequently been suggested.

The purpose of this project is to investigate the clarification of colloidal suspensions using cataphoresis to assist gravitational sedimentation in a thickener.

PREVIOUS APPLICATIONS OF CATAPHORESIS

There have been many research projects done on the application of cataphoresis to the dewatering or concentration of colloidal suspensions. Some of these projects have led to the construction of full scale industrial processes which employ cataphoresis, while others have prompted the construction of pilot plant models. The majority of the work ended after laboratory tests as scale up proved the systems to be uneconomical. Of the processes which have found application in the industry, almost all of them are in the European clay refineries, while in North America there are no examples of industrial usage of cataphoresis for treating colloidal suspensions.

The pioneer work of Count von Schwerin* in Germany in 1900 which involved the dewatering of peat electrically was the first industrial application of electrokinetics. Schwerin's work led to the development of the rotating-anode electrophoresis machine which was used in several kaolin refineries in Czechoslovakia and Germany. Essentially the machine is a drum type filter with the drum acting as the anode and a cathode is placed in close proximity to the drum in the slurry tank. These developments sparked

*B. SCHWERIN developed the electro-osmose filter press for electrically dewatering ball clay, kaolin and peat. U.S. Patent 1,133,967 (1915)

American interest in cataphoretic applications which peaked in the early 1940's and resulted in numerous publications. Two scientists, who were with the U.S. Bureau of Mines in Norris, Tennessee, Sidney Speil and M.R. Thompson are probably the best known Americans who have worked in this area. Speil and Thompson concerned themselves primarily with the dewatering of clays using cataphoresis. They were interested in both clarifying the suspension and dewatering the deposit but their main interest lay with the characteristics of the deposit, which is a reversal in priorities when compared to the current research. All their work was carried out in the laboratory using cataphoresis in the horizontal plane. In several publications (1,2,3) they summarized the results of these tests to illustrate how the treatment of the suspension could best be done. There is one conclusion which they reached which is of special interest since it was perhaps the first suggestion that cataphoresis be used to aid gravitational sedimentation. It is reproduced here:

"For minimum power consumption, the cataphoretic migration should be downward to utilize, and not to oppose gravity sedimentation; in any event some non-electrical method should be used to aid the movement of particles from the cathode to the anode." (2)

The publications of Speil and Thompson led to the study of dewatering colloidal suspensions, using the rotating-

anode electrophoresis machine, by other investigators. Two such studies^{4,5} which were done proved the system to be uneconomical because of the high power consumption. Again, these studies were directed at the moisture characteristics of the deposit and not the clarity of the water fraction. One of them⁵ had reached the pilot plant stage before being rejected and is perhaps the closest that cataphoretic techniques have come to actual industrial operations in North America.

The net result of all this research is an abundance of publications* but, as yet, there are no industrial processes developed which use cataphoresis by itself, or as an aid, to clarifying colloidal suspensions in North American industry.

*A more complete bibliography is found in: Poole: J.B., Doyle: D., Solid-Liquid Separation, Swindon Press Ltd. for Her Majesty's Stationery Office, London, England 1966 pg. 842 - 44.

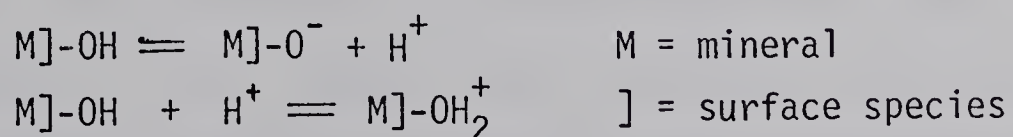
THEORETICAL REVIEW

A: The Origin of the Charge at the Mineral-Water Interface

The origin of the charge at the mineral-water interface is of obvious importance in mineral processing, since a large amount of the flotation, rheological and aggregation behaviour of mineral pulps is influenced by this charge. Much of the understanding of the charging mechanism at the mineral-water interface has been developed from the results of electrokinetic measurements of the zero-point-of-charge and of the effect of potential determining ion concentrations on the zeta potential. Several theories have been developed to explain the origin of this charge on various classes of minerals.⁶ In this project silica and clays of the zeolite type silicates were used and as a consequence only the theories directly related to these minerals are presented.

Silica Charging Mechanisms

For a simple oxide mineral such as silica, hydration of the 'broken bond' surfaces has been postulated as a source of surface charge to explain why H^+ and OH^- are potential determining ions. The mechanism may be written:



An alternative charging mechanism, proposed by Parks and DeBruyn,⁷ involves the adsorption of charged hydroxo complexes of the form $M(OH)_n^{z-n}$ where z is the valency of the metal and n is an integer. These metal hydroxo complexes are derived from the hydrolysis products of material dissolved from the surface, i.e. from amphoteric dissociation of $M^{z+}(OH)_z^{-(aq)}$. Since the concentration in solution of both these complexes is pH controlled, electrokinetic measurements do not permit selection between these two charging mechanisms.

Clay Charging Mechanisms

Van Olphen⁸ and Parks⁹ have discussed the formation of surface charges that result from lattice substitutions in the bulk of the solid. The classical example of such substitution is the clay minerals in which substitution of aluminum (Al^{3+}) for silicon (Si^{4+}) and magnesium (Mg^{2+}) for aluminum produces a net negative charge in the clay lattice. This charge dominates the sheet surfaces of the clay minerals, which in contrast to the edges, do not present 'broken bond' surfaces. The edges of the clay lattices are considered to behave in the same fashion as the 'broken bond' surfaces of the simple oxides with H_3O^+ and OH^- being potential determining ions. The combined result of the 'broken bond' surfaces and the negatively charged sheets on kaolinite is a particle whose point-of-zero charge⁹ is around a value of pH equals 3 to 5 but whose edges may be positive at a value of pH equals nine.

Bentonite minerals usually display negative zeta potentials at all pH values indicating that the negative charge resulting from lattice substitution dominates the charging mechanism of the particles. Both kaolinite¹¹ and bentonite¹² show a relationship between particle size and surface charge with the measured zeta potential increasing for decreasing particle size in the range studied. There is little doubt as to the charging mechanism of the sheet surfaces in clays but again selection cannot be made to determine the charging mechanism at the lattice edges.

B: Electrical Double Layer Theory

The very basis of this investigation is the migration of a charged particle under an applied D.C. voltage gradient. The migration depends on the characteristics of the double layer formed at the mineral-water interface as a result of the charge formed there.

Surface Chemistry of the Interface

Most substances acquire a surface electric charge by ionization and/or by the adsorption of ions when brought into contact with the polar, aqueous medium. There have been several models advanced to explain the surface chemistry of the interface.

The potential difference which develops across the mineral-water interface, since electricity is atomic in nature, may be conveniently pictured as an electrical double layer. One phase acquires a net negative charge (excess of electrons), the other a net positive charge (deficiency of electrons), while the system as a whole retains its electroneutrality.

The first quantitative discussion of this double layer was given in 1897 by Helmholtz.¹³ He postulated a rigid array of ions of opposite charge to the surface adsorbed on the surface (much like a parallel plate capacitor). Such a rigid array could scarcely be permitted by the thermal motion of the liquid consequently for this

and other reasons* the model proved to be inadequate.

Gouy later put forward a new model which considered the solution side as a diffuse layer of ions in equilibrium with the field of the surface and the thermal kinetic forces of the solution.¹⁴ This theory also proved to be inadequate because it did not lead to a connection between capacity and potential as evidenced by experiment, and, the inherent assumption of point charges lead to absurdly high ionic concentrations near the surface. In 1924 Stern proposed his "diffuse double layer" which incorporated both the compact Helmholtz layer and the diffuse or Gouy-type layer. Grahame later modified the Stern model to produce the Stern-Grahame model of the electrical double layer. This is the model which is most widely used today in mineral processing publications. Unfortunately, it has a number of faults which had to be corrected.** Toward this end, Bockris, Devanathan and Muller¹⁵ developed a model of the double layer which is, to date, the best representation of the surface chemistry of the water-mineral interface.

The model which arises from the Bockris, et al, theory is schematically illustrated in Figure 1.

*For further discussion see (13) Sec. 9.22 and the Debye-Huckel atmosphere. The model was unsatisfactory because it predicts a constant capacity with changing potential, contrary to experiment.

**Reference (14) has a detailed discussion of all models in present use including criticisms of them.

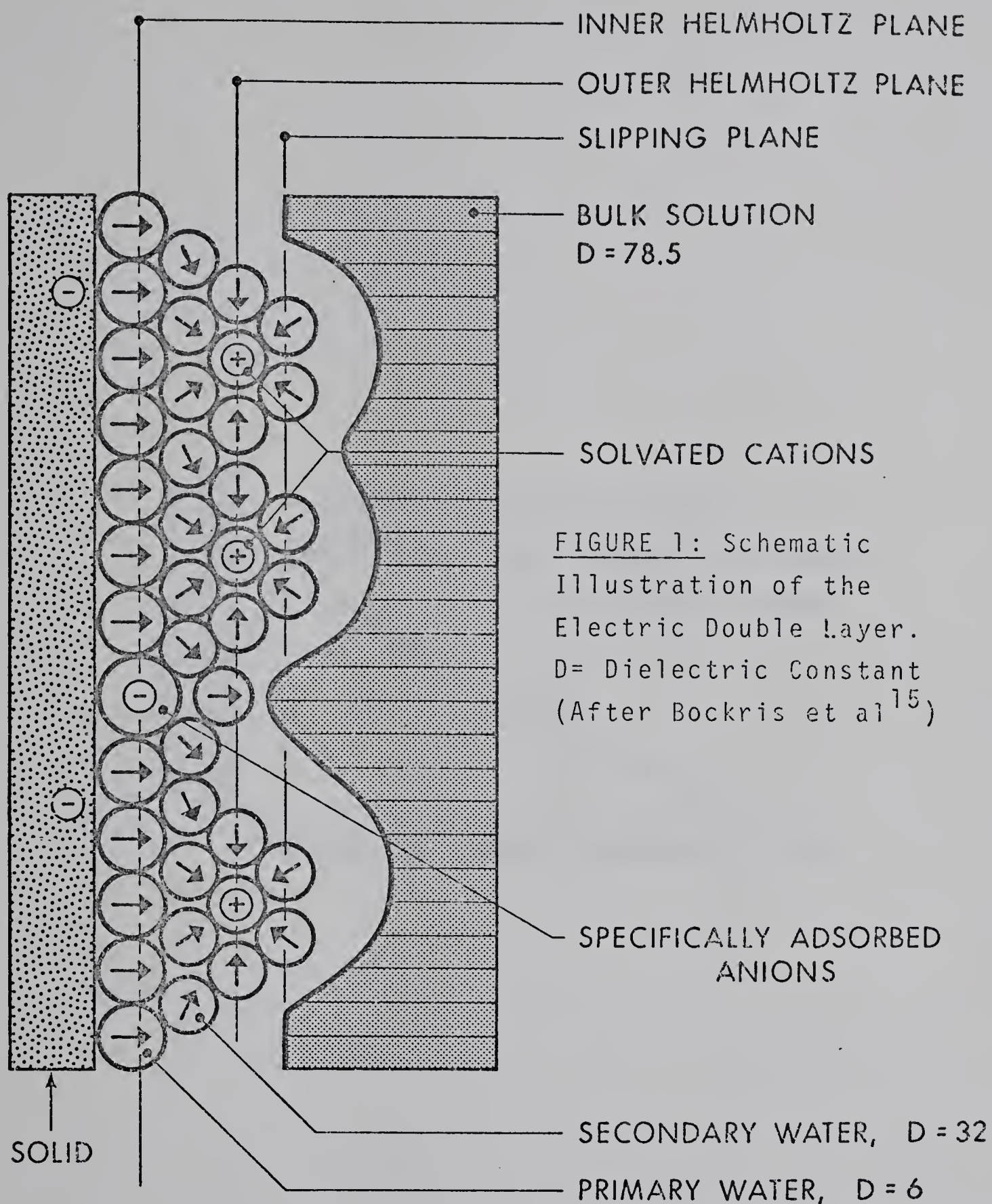


FIGURE 1: Schematic Illustration of the Electric Double Layer. D = Dielectric Constant (After Bockris et al¹⁵)

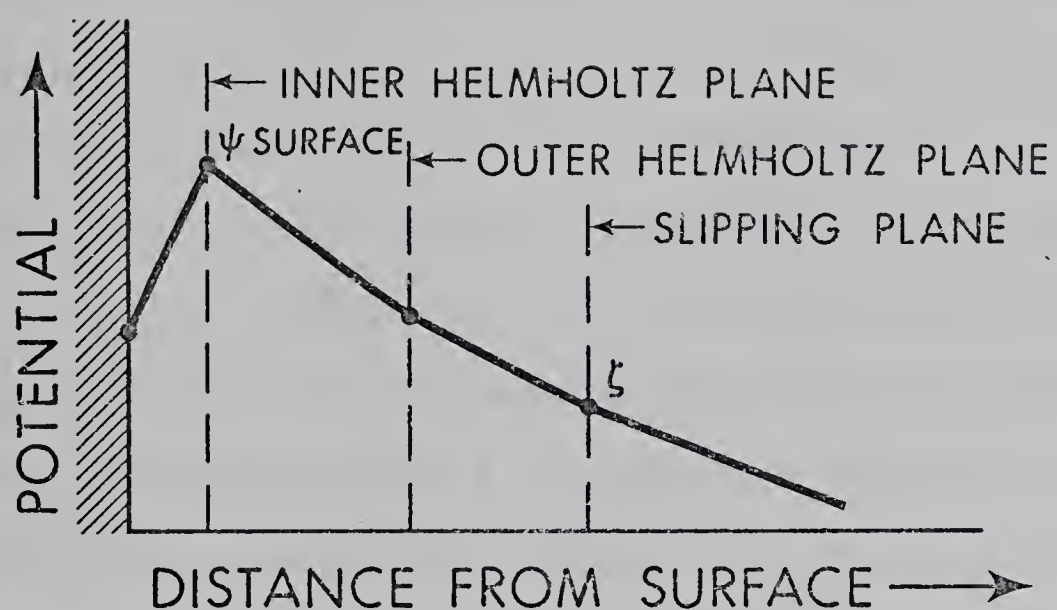


FIGURE 2: The Variation of Potential With Distance From The Solid Surface When There Are Potential Determining Ions Distinct From the Surface (After Adamson²⁴)

Figure 2 illustrates the variation of potential with distance from the interface, for this model. It is necessary at this point to define the electrokinetic potential (zeta potential) which is shown on Figure 2 as ζ . The zeta potential (ζ) may be defined as the potential at the plane of shear (or slipping plane) between the fixed layer of liquid adjacent to the surface and the liquid constituting the bulk of the solution. This definition is used by most authors in discussions of electrokinetic theory. Those aspects of the definition of zeta potential which are of most interest are:

- i) The location of the slipping plane within the double layer since this will be a factor in the magnitude of the zeta potential, and, ii) The magnitude and sign of the surface potential since in a given aqueous solution the zeta potential depends on this value. The zeta potential is a complex function of all the species present in the medium.

Figure 1 deserves further explanation. Basically there are four areas which can be looked at separately. Firstly, the surface of the solid and its chemical composition determine which are the 'classical'* potential determining ions that may specifically adsorb to the surface in such a manner as to actually become the new surface and hence determine the solid surface potential.

*For example OH^- and H_3O^+ are classical P.D. ions for SiO_2 since they interact with the surface but it will be shown later that Cl^- from KCl can act as a P.D. ion.

This qualification is made to distinguish the ions which are 'classically' defined as being potential determining from those potential determining ions which specifically adsorb on the surface forming the inner layer as shown on Figure 2. This second area, the inner layer, may appear at first glance to be incorrect from Figure 1 since it is electrostatically unfavourable to have anions adsorbed on a negative surface (this will be discussed in some detail later). The combination of the classical and non-classical specifically adsorbed ions, then determines the potential which can now be defined as the surface potential and it is this value upon which the zeta potential depends. The third area is the Helmholtz layer which consists of non-specifically adsorbed, hydrated ions, opposite in charge to the surface. They are held in this layer by fairly strong electrostatic and nonspecific (e.g. Van der Waals) chemical forces. This layer may be thought of as being rather immobile in the sense of mobility normal to the surface, since, if the adsorption forces are strong, the lifetime of the ion in the layer will be rather long. The mobility of these ions, normal to the surface, is important since it determines the location of the slipping plane. Loosely held ions can result in the slipping plane being located in the Helmholtz layer while strongly held ions will cause the plane of shear to be located outside this layer. Finally there is the Gouy or diffuse layer which is populated by a diffuse

distribution of positive and negative ions, those having a charge opposite the surface potential being in excess. Figure 2 shows the potential variation with distance for a system having the shear plane located in the diffuse layer. In the interests of semantics this should then be called the electrical triple layer theory but since this definition is of little importance in the current research the name electrical double layer will be retained.

It was previously mentioned that Figure 1 might be interpreted to be in error by showing anions specifically adsorbed to a negatively charged surface. The explanation for this inner layer formation is based on the hydration of ions. (Ref. 15. ⁵) Primarily hydrated ions - those which are associated during transport with a definite number of water molecules - tend to be less specifically adsorbed than those which are not so hydrated. It has been shown¹⁴ that for alkali metals, all the monovalent cations from Li^+ to Rb^+ possess primary hydration shells, while Cs^+ and Fr^+ do not. Similarly, F^- is hydrated to a degree similar to that of an alkali metal cation possessing a primary hydration shell, but, larger halide anions can be regarded as not being hydrated.

In summary, ions tend to be specifically adsorbed if they are bereft of a primary hydration sheath; for ions of a given family (e.g. halides), the specific adsorption is greater as the ionic radius increases. Specific adsorption is not a phenomenon restricted to anions and provided

the cation is sufficiently large it adsorbs to a super equivalent extent.

Thus, if ions have sufficiently stable primary hydration shells they will not be specifically adsorbed. Such nonspecific adsorption of ions into the Helmholtz layer is frequently called 'equivalent'. If the ion possesses no primary hydration water, it can gain energy by replacing the surrounding water dielectric with the dielectric of the surface (provided the surface dielectric approaches infinity), and move out of solution into contact with the surface. The tendency to do so is not dependent (primarily) upon the charge of the surface and may occur against it if sufficient energy is to be gained. Such adsorption is best termed "super equivalent".¹⁶

The surface chemistry of the interface can be represented to a good qualitative approximation by the Bockris, Devanathan and Muller (B.D.M.) model of the electrical double layer.

Zeta Potential and Particle Mobility

In this work the magnitude of the zeta potential is important because it determines the rate of migration under an applied D.C. voltage gradient. The zeta potential as defined, cannot be directly measured and must be calculated from mathematical equations which contain variables that can be measured. One such equation, (1) which is commonly used and is derived elsewhere,¹⁷ is the Smoluchowski

equation which relates the measured particle mobility to the zeta potential.

$$\xi = \frac{4\pi n u_m}{DE} \dots\dots\dots [1]$$

where ξ = zeta potential
 n = viscosity of the bulk solution
 D = dielectric of the bulk solution
 u_m = the particle velocity
 E = voltage gradient.

The mobility of the particles, as determined by the magnitude of both, the zeta potential and the voltage gradient, is important. Since the mobility is the essential factor in this research all discussions will concern the mobility without calculating zeta potential. The means of determining mobilities is the microelectrophoresis cell, which is described in the experimental apparatus. A particle is placed under a known voltage gradient and the time it takes to travel a certain distance is recorded. From this data the mobility is calculated and a typical value would be; -3×10^{-4} cm/sec volt/cm, where the sign is determined by which electrode it migrates toward, in this case the anode.

The Effects of Electrolytes on Zeta Potential

The effects of different electrolytes on zeta potential and, consequently mobility, are extremely important in natural systems where the medium is other than distilled water. In the way of an explanation of these effects an illustrative example taken from actual tests will be given.

Figure 3 shows the relationship of a dilute suspension

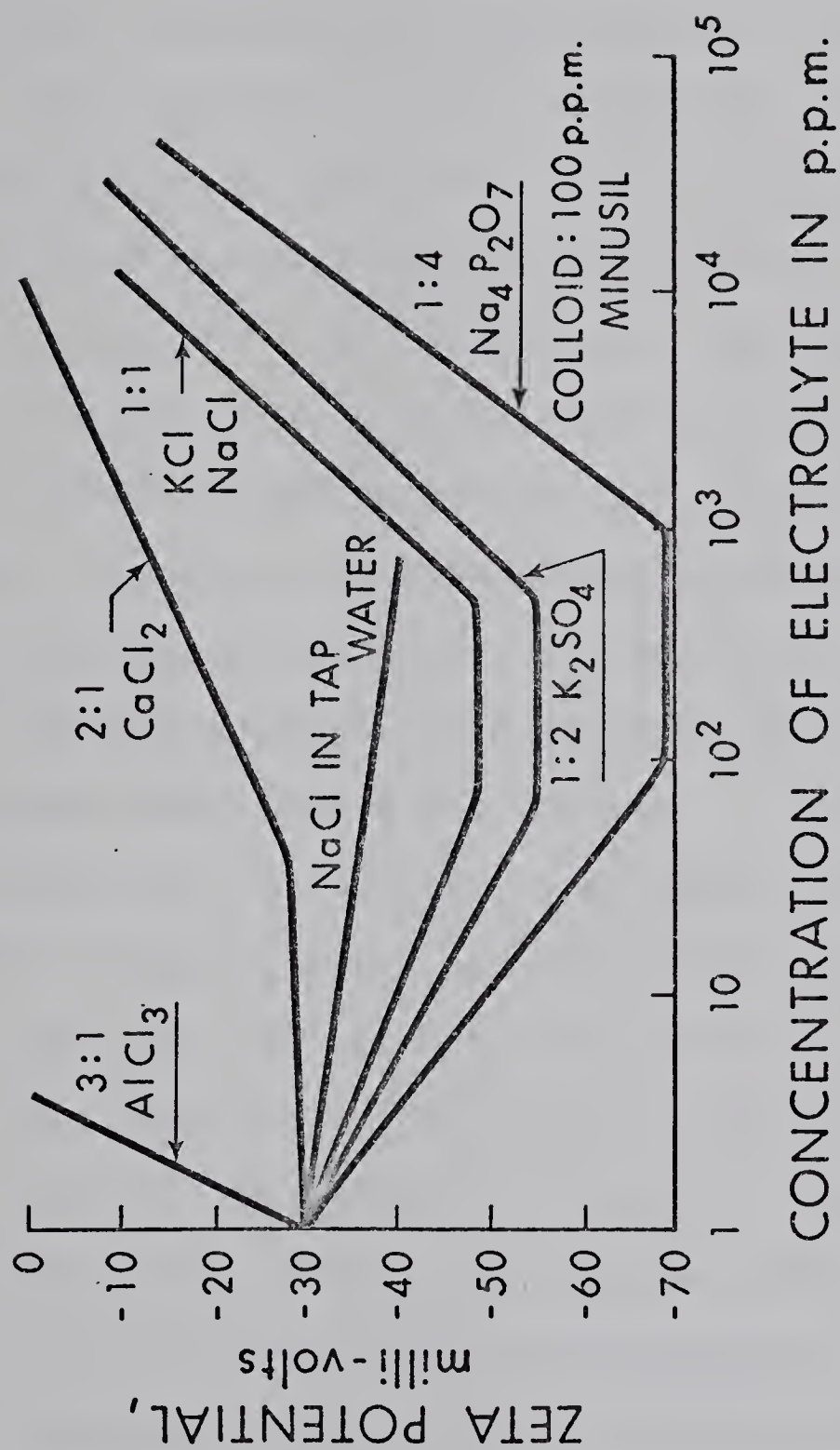


FIGURE 3: The Effect of Different Electrolytes
On the Zeta Potential of a Silica Colloid

of minus five micron silica in the presence of different electrolytes at various concentrations. At a concentration of 3ppm of the electrolyte, the measured zeta potentials reflect some interesting relationships between the electrolytes, specifically, the valence of the cation and the zeta potential. Even as the ratio of the number of cations to anions decreases in the going from NaCl to CaCl₂ to AlCl₃ the zeta potential decreases. (Calculations show that there are fewer cations per unit volume in the sequence $\text{AlCl}_3 < \text{CaCl}_2 < \text{NaCl}$). All of these cations possess primary hydration sheaths and are all equivalently adsorbed. Therefore, in the ability to compress the double layer and hence reduce zeta potential, trivalent cations are much stronger than divalent which in turn are much stronger than monovalent cations. (Compression of the double layer means that there is a larger potential drop across the Helmholtz plane as illustrated in Figure 2). Schulze and Hardy demonstrated this trend in 1880 when studying the flocculation of pulps by reducing zeta potential and allowing agglomeration to occur. They found that divalent cations were 25 to 75 times as effective as monovalent cations in coagulating electronegative colloids, and that trivalent cations were more effective than divalent, in this ratio. Thus, even though the superequivalent adsorption of Cl⁻ results in greater absolute surface potential in the AlCl₃ dispersion the Al³⁺ ion is far more effective in 'shielding' this potential with respect to the

other two dispersions. The same holds for Ca^{2+} as opposed to Na^+ . In conclusion the valence of the cation is extremely important in determining the magnitude of the zeta potential. There appears to be little difference in zeta potential if the electrolytes have the same stoichiometry as demonstrated by the curve(s) for NaCl and KCl.

Another very interesting feature of Figure 3 are the curves for the electrolytes with monovalent cations and polyvalent anions. It is evident that as the anion charge increases the zeta potential decreases for electrolyte concentrations less than 50ppm. This is a result of the superequivalent adsorption of the anions, of which, those with the largest valence result in the largest absolute value of the surface potential. This trend is easily understood using the B.D.M. model of the double layer.

Perhaps, what is more interesting, is the shape of those curves for electrolytes with monovalent cations. They all show an initial increase in the absolute value of the zeta potential, followed by a 'plateau' which in turn is followed by a decrease in the absolute value of the zeta potential. This characteristic shape led Riddick¹⁸ to postulate the 'Bulk Stress' theory. In its most simplified form this theory states that for dilute suspensions ($\leq 10\%$ solids by weight) preferential adsorption (superequivalent) of the anions takes place until a monolayer is formed around the particle. After monolayer

formation, the colloid can then gainfully, as far as zeta potential is concerned, accept no more of the anion of dispersant. Hence, further additions of the reagent result in its build up solely in the bulk of the solution. Since zeta potential is defined as the potential between the plane of shear and the bulk of the solution, a build up in the bulk will cause a decrease in the absolute value of the zeta potential. The plateau during build up, is common only to dilute suspensions and for concentrated slurries a peak is reached with immediate reversal (see 17, Fig. 25 and pg. 110).

These are the effects of electrolytes on zeta potential and mobility which are of most importance in the current research.

Equilibration of the Zero Point of Charge

Figure 3 shows that at some value of electrolyte concentration, there is no measurable zeta potential. This is called the zero point of charge (Z.P.C) or the Isoelectric Point (I.P.). It is common to find Z.P.C. quoted at a certain pH, for example, if silica is immersed in distilled water for one day the Z.P.C. occurs at $\text{pH} = 2.8$.¹⁹ It requires some time for the double layer to equilibrate with the bulk of the solution and as a result a variation of Z.P.C. with aging time in water is observed.¹⁹ For silica, the equilibration is essentially complete in 24 hours (18 Fig. 3). The Z.P.C. equilibration time for zeolite type silicates could not be found in the literature and a value of 24 hours was arbitrarily chosen for these minerals.

The theory contained in the preceeding discussion of the electrical double layer is sufficient to rationalize the experimental results. There are several excellent publications^{14,20,21} which deal with the complexities of the double layer, including the effect of surface curvature and the mathematics. Publications^{13,22,23,24} which give the basics of double layer theory are also available.

C: The Principles of Cataphoresis

The magnitude of the zeta potential determines the migration rate of the colloid under an applied D.C. voltage gradient, this migration process is known as cataphoresis.

Generally, the term electrophoresis is used to describe migration process where a charged particle moves, relative to a stationary liquid, under an applied voltage gradient. The process is usually given different names depending on the size and/or type of particle involved. If the particles are small ions the phenomena is known as ionic conductance, if they are larger molecules, such as proteins, it may be called electrophoresis, and, if they are of colloidal size, it may be called cataphoresis.

The basic principles of cataphoresis are relatively simple. When a charged particle is placed in an electric field created by an applied voltage it will migrate toward the electrode which has the opposite charge of the zeta potential. The ions within the slipping plane will remain attached to the particle, that is to say the zeta potential will remain constant during migration, while the ions in the layer outside of the slipping plane will be partially swept away causing a distortion of this layer. If the same charging mechanism was at work on all the exposed surface of the particle the migration rate will be independent of size. This is evident from

equation 1, since no particle diameter term is included. If, however, the charging mechanisms are different and have acted on approximately the same amount of surface, then different zeta potentials are obtained with respect to a particle where one charging mechanism dominates.^{11,12}

There are, of course, a number of complications in the more detailed theory of 'electrophoretic' motion.^{25,26}

The effective viscosity in the diffuse double layer is affected by the fact that the ions in it are also moving due to the electric field; since the ions which are in excess in this layer are those which are oppositely charged to the zeta potential, this gives rise to "electrophoretic retardation". These ions entrain solvent with them (e.g. through their hydration shells and ion atmospheres), so that there is a local motion of the medium opposing the motion of the charged particles. There is also a relaxation effect in that, due to the motion of the particle, the double layer lags somewhat behind, and, again, the effect is one of retarding the motion of the particle. Another consideration is that the double layer region is a source of conductance as is the surface of the particle itself. The last complication is difficult to evaluate and for reliable zeta potential measurements nonconducting surfaces or particles are necessary.

These three complicating factors are difficult to assess in a system such as that being used in these tests, although, the relaxation effect is thought to be the largest

contributor since the other two are dependent, to some extent, on the ionic strength of the medium and the tests are performed with low ion content. There are many in depth reviews of 'electrophoretic' theory and its measurement, techniques and applications, available in the literature.^{6,22,23,24}

D: Basic Thickener Theory

The thickener, from outward appearances, seems a simple machine for concentrating solids in a solid-fluid feed but the mathematics of particle settling within a thickener are exceedingly complex and not well understood. At present, thickener design is carried out by running laboratory batch tests and then using these results and the method of either Coe and Clevenger²⁷ or Talmadge and Fitch²⁸, to determine the size of thickener required for a given application. These methods are of obvious value because they allow the engineer to size the thickener from a few simple laboratory tests but they do not work in all cases. Many skillful researchers have worked on the problem and a great deal more is known about sedimentation than in the past, but, as yet, there is no one theoretically solid and satisfying way of predicting thickener performance completely and accurately from measurements made on laboratory batch tests. At present, most of the studies are being done on the laboratory batch tests²⁹ (settling in a tall cylinder) and mathematical models of subsidence rates³⁰ have been developed. Unfortunately, little is known about the internal workings of a continuous thickener.

The particle velocity within a continuous thickener has four contributing components. These are:

i) The gravitational settling velocity component:

This is determined by a force balance where the gravitational force causing the particle to settle is offset, to some degree, by the buoyancy effect resulting from displacement of liquid by the particle, and, the frictional resistance from the relative motion of the particle and the liquid. It is also a function of the local particle concentration.

ii) The velocity component due to the upward movement of water to the overflow discharge: This component is a function of both depth and radial position in the thickener (depending on where the zones are located). It is further complicated in the equipment used in the research, by replacing the conventional continuous rim launder for overflow collection by four discrete discharge ports.

iii) The velocity correction component: This component is used to account for all other contributors to the net velocity. These contributors will include short circuiting, thermal currents, currents created by a density gradient between the feed in the well and the 'clear' water outside (this presupposes the clear water layer to be below the level of the first feed well discharge port).

In a conventional thickener these three terms comprise the net velocity of a particle settling within a thickener. Thus it can be seen that the velocity of a particle is complex three dimensional function of position in thickener.

When cataphoresis is used to aid gravitational sedimentation a further component is added:

iv) The cataphoretic velocity component: This is a function of the magnitude of both the zeta potential and the applied voltage gradient in the thickener.

The complexity of the net velocity of a particle in the system disallows any mathematical treatment of sedimentation in this work. The flow patterns within a thickener are ill-defined but depend on the feed rate and location of the zones.

The purpose of this project is to apply cataphoresis to increase the settling velocity of the colloidal particles, in the floc bed zone, such that they report to the underflow which they would otherwise not do. In the absence of a sound mathematical treatment this qualitative thickener theory adequately describes what occurs in the system.

A more complete discussion is available in the literature,³¹ but a greatly simplified qualitative summary of thickener behaviour can be stated as: The normal conception of thickening is probably that the pulp enters the feed well where turbulence is quieted and then emerges to assume a radiating path on its way to the overflow discharge, dropping out the solids under the influence of free settlement. Thereafter the mechanism of thickening is supposed to follow the pattern of behaviour of stationary pulps in tall cylinders.^{27,28.29}

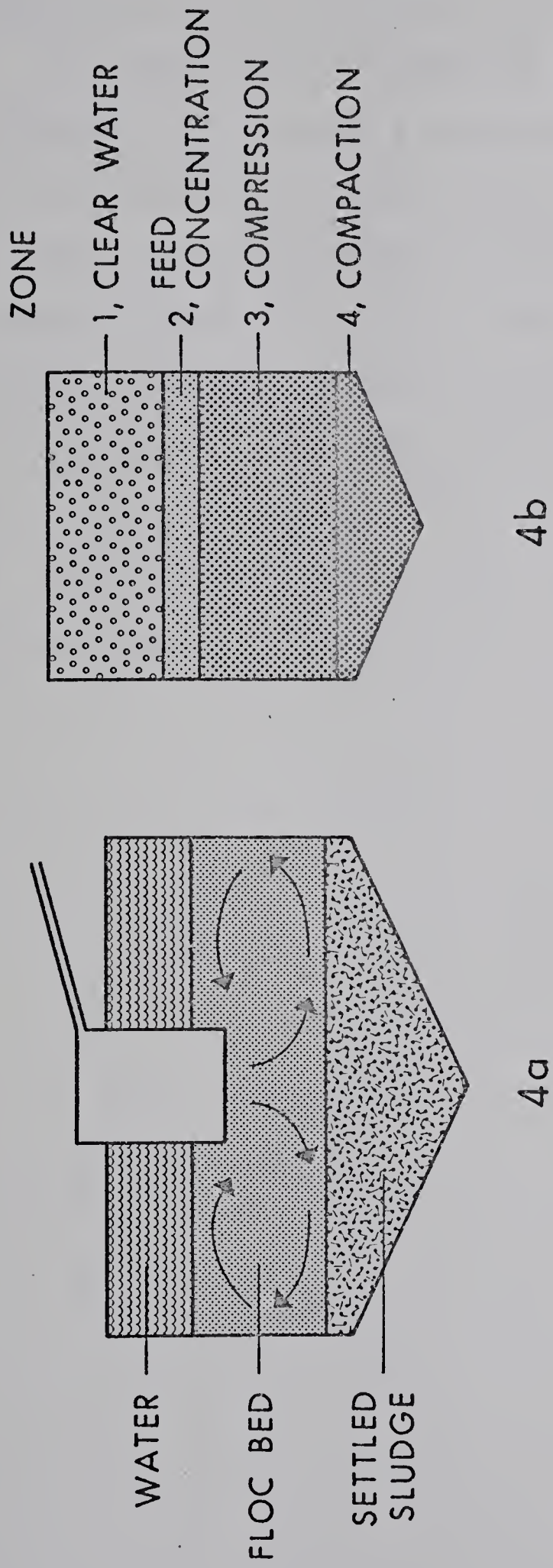


FIGURE 4: The Zones Occurring In a Continuous Thickener Operated Within Capacity

Throughout this discussion the term "zones" has been used. To clarify what is meant by this term, Figure 4a is presented. As long as a thickener is operated well within its designed capacity there exist three distinct zones with a sharply defined boundary between floc bed and settled sludge.³¹ The floc bed is the area in which settling is supposed to occur according to laboratory tests in tall cylinders. The floc bed actually consists of two zones as shown on Figure 4b³² as the second and third zones. This second zone of feed concentration is extremely thin and frequently it cannot be detected.

EXPERIMENTAL

A: Materials

There were three different materials used in the test program. Silica, bentonite and a sample from the Great Canadian Oil Sands (G.C.O.S.) plant at Fort MacMurray in northern Alberta were obtained. The G.C.O.S. sample will be described under the experimental results and discussion for that test. Table 1 gives the major characteristics of both the silica and bentonite used in testing.

.....

Table 1: Characteristics of Silica and Bentonite.

	<u>SILICA</u>	<u>BENTONITE</u>
Brand Name	-400 Mesh Silica Flour	Alberta Bond Canadian Bentonite
Source	Ottawa Silica Company, Ottawa Illinois, U.S.A.	Baroid of Canada Onoway, Alberta Canada
Dry Density	2.59 gm/cc	2.7 gm/cc ⁽³³⁾
Density in Water	2.59 gm/cc	2.07 gm/cc
Specific Surface Mean Spherical Diameter	4.4 microns	6.2 microns
Chemical Formula	SiO ₂	Al ₂ Si ₄ O ₁₀ (OH) ₂ ·xH ₂ O ³³

.....

The wet densities were determined from pyknometer measurements and the size data obtained by Fisher Sub Sieve Analysis (air permeability). The other characteristics, specifically mobility in water and slurry concentrations will be included with the test results.

B: Experimental Apparatus

The thickener apparatus which was designed and built for this project is illustrated both schematically and in pictures in Appendix 1, Figure 22 and Plates 1 through 4.

Thickener System

The apparatus consists of a two foot diameter lucite thickener tank with an adjustable overflow withdrawal system, at discrete levels, through four spigots. The feed well was fabricated from four inch I.D. polyvinyl chloride (P.V.C.) tubing. It has forty-four one inch holes drilled in it which allow the feed slurry to enter the thickener tank. (This particular design was adopted from the Cross⁴ theory which says that wells of this design increase the thickener capacity.) The thickened slurry is removed from the bottom of the thickener tank by means of a set of rakes rotating at one R.P.M. The rakes were also constructed from P.V.C. and feature blades which are at a 65 degree angle to the longitudinal axis of the rake arm, and, are rubber tipped to minimize damage to the tank bottom during continuous operation. Within the thickener, the cataphoretic action is obtained by the installation of two electrodes. The bottom of the thickener tank is a paraffin-graphite mixture (area 3000 cm^2) and, for the solid materials used in testing, served as the anode. The upper electrode (cathode: total area 2500 cm^2) was made from a

fourteen mesh brass wire screen. The cathode is held rigid by a P.V.C. collar with six radial arms to which the screen is attached by a brass wire.

The cathode is suspended in the thickener by insulated, thin guage copper wires which are attached to the collar arms and an appropriate overflow spigot. The essential features are the transparency of the tank and that between the electrodes, all parts are non-conducting plastics. A thermometer with a reading accuracy of $\pm 0.03^{\circ}\text{C}$ is suspended with the bulb just above the cathode. There is a lucite fitting, called the consolidation chamber, which reduces the three inch discharge port in the anode to half inch which is suitable for attachment to the tygon tubing used in the under flow pumping system. The four spigots, being used to collect overflow, are connected to the sampling tray by jayon tubing and all other spigots are stopped with corks. Through two of these corks there are stainless steel wires which lie in the same vertical plane. A voltmeter is connected to these probes such that any internal change in the thickener, when the power is on, is noticed immediately.

The feed is withdrawn from the reservoir tank under a gravity head with the flowrate being controlled by the primary control valve. The feed line is one inch I.D. jayon tubing and it discharges to the feed tank. Both the reservoir and feed tanks are equipped with mixers to ensure good particle size representation in the feed slurry. Once

in the feed tank the slurry either by-passes to the return pump or is pumped through a variable speed peristaltic pump to the feed well. The underflow pump is also a variable speed peristaltic pump with its discharge in the sampling tray. The overflow, underflow and by-pass streams are recombined in the centrifugal return pump and go to the reservoir tank. Upon discharge to the reservoir tank the return slurry passes through a 48 mesh bucket screen to remove scale and other large objects, which appear infrequently. The reservoir tank is fitted with a refrigeration system which attempts to offset the heat input to the slurry from the mixers and pumps (≈ 8.5 h.p.) and the resistance losses in the thickener tank (≈ 250 watts). An antifreeze water mixture is cooled by freon and pumped through 50 feet of 3/8 inch I.D. copper tubing located near the reservoir discharge.

The power source used to apply the voltage gradient across the electrodes has maximum input values of 150 volts and/or two amps, whichever comes first. The source is fitted with two "Selectest" multifunctional meters one of which measures current and the other voltage.

This is the system used for continuous clarification tests.

Batch Testing

The apparatus for batch testing was simply a 1000 ml beaker fitted with the same electrode configuration as described above. In this case the brass screen cathode

was attached to a piece of styrofoam and allowed to float near the suspension surface. The power source was a constant voltage D.C. supply capable of up to 500 volts with a maximum current of 500 milliamps.

Mobility Measurement

The apparatus used for mobility measurement is shown in Appendix 1, Figure 23 and is fully described elsewhere.¹⁷ There is one difference, that being, in this case, the power source used in batch testing, replaced the electrophoretic mass transport analyser.

C: Experimental Procedure

The basic experimental procedure is outlined below while minor procedural changes in the clarification tests are included with the discussion of experimental results.

Clarification Tests

A slurry of the desired solids content was mixed in 450 pounds of water, either tap water or demineralized water as recorded in the results. The slurry was mixed for approximately one-half hour and then the mixer turned off and the mixture allowed to sit for 24 hours. If any chemicals were to be added to the system this was done so during the mixing.

At the beginning of a run the reservoir tank mixer and refrigeration equipment were turned on and allowed to run for about one-half hour before feed was withdrawn from the tank. To fill the thickener, the rakes, underflow pump, and return pump were turned on and the feed line from the reservoir was placed on the thickener. When an overflow was obtained the primary control valve was shut off and the feed line drained and transferred to the feed tank. (In some tests the power was turned on immediately after the slurry level in the thickener was above the cathode). The primary control valve was opened and the feed pump and feed tank mixer were turned on. Using the primary control valve a suitable by-pass stream was obtained. This prepared the system for testing.

To initiate a test an overflow flowrate (Q_o) was chosen along with an underflow solids concentration (S_u). Adjustment of both the feed flowrate (Q_f) and the underflow flowrate (Q_u) allowed these chosen values to be attained. During this 'run-in' period the four variables above and the temperature in the thickener were monitored as a function of time from the time of test initiation. When both Q_o and S_u had reached the desired values, the actual testing was begun. At this time the overflow solids concentration (S_o) was monitored. The determination of S_o was done at a minimum of one-half hour intervals. Three consecutive S_o values which were of about the same magnitude and showed no trend meant the system had reached steady state (typically ± 0.02 per cent solids by weight).

When steady state was reached, then, according to the object of the test, a change was made to one of the major independent operational variables. Monitoring of all variables was continued and the system was followed to steady state by the procedure above. (The monitored variables provide the record of the system performance.) After reaching steady state another change to the independent variable under investigation was made. When the test was completed the primary control valve was shut off and the slurry allowed to return to the reservoir tank. The slurry was then fed to several tubs where the solids were allowed to settle for 24 hours. The water was then

decanted to the drain and the solids discarded. After draining the whole system everything was cleaned with tap water and all the equipment turned off. Motors were oiled and the apparatus prepared for the next test.

Determining Variable Values

The methods for determining Q_o , Q_u , Q_f , S_u and S_o are described in this section.

Flowrates were the easiest to measure. To determine Q_o and Q_u the appropriate discharge lines were allowed to drain into a graduated cylinder for one minute. Q_f was determined by summing the values for Q_o and Q_u . The time required to determine all three variables was about five minutes since in most cases two readings for each of Q_o and Q_u were taken and the mathematical averages reported.

The determination of S_o was perhaps the most complex operation. Investigation of light transmittance and weighing techniques for determining the solids concentration by weight in the overflow proved the latter to be the most accurate. The method of sample preparation was as follows: Samples of the overflow were withdrawn into two 100 millilitre volumetric flasks insuring that the pulp level was above the mark. The flasks were removed to a sink and stoppered. One flask was then shaken vigorously while being inverted. The stopper was immediately removed and a 20 millilitre pipette passed down through the pulp and back during which it is withdrawing some slurry. The pipette was

then raised and enough slurry allowed to return to the flask to make up to the mark. This complete operation takes approximately one minute to complete. The procedure was repeated for the second flask and then both were stoppered and the outside thoroughly cleaned. Once complete, the flasks were taken to the balance room. A cotton swab wrapped with absorbent tissue was inserted in the neck of the flask and the neck dried. One flask was weighed and immediately thereafter the temperature was taken with a thermometer which is accurate to ± 0.25 degrees centigrade. The second flask was then weighed, both being done on a Saggitarious Model 2642 balance with a reading accuracy to 0.0001 gram. The pulp densities were determined and together with the temperature were recorded. The actual calculation for determining S_o is given following the next section.

The determination of S_u was done in different ways for different tests. In general if S_u was less than 18 per cent the technique described for S_o above was used however if S_u was in excess of this value a simplified technique was applied. A sample of the underflow was obtained in a graduated cylinder such that the slurry volume and weight could be reported almost directly. Cleaning precautions were taken with this technique as well but the balance used was of the Torsion type and accurate to 0.05 gram. The corresponding temperature was obtained from the thermometer in the system although the calculations are relatively temperature insensitive when dealing with S_u values in

in excess of 18 per cent.

The equation for determining the percentage solids by weight in a thickener discharge is derived below.

Let X = mass flowrate of water in the discharge
having a temperature sensitive density = P_w

Y = mass flowrate of solids in the discharge
having a density = P_s

Z = mass flowrate of the discharge pulp having
a reported density = P_p

then $Z = X + Y$ is the mass balance[2]

and $Z/P_p = X/P_w + Y/P_s$ is the volume balance[3]

it is required to find (Y/Z) 100%

by rearranging [2] and substituting into [3] to eliminate X the following equation is obtained.

$$(Y/Z) 100\% = (P_p - P_w)/(P_s - P_w) (P_s/P_p) 100\% \dots\dots[4]$$

Since for any given solid-water system P_s is known and P_w can be determined when the temperature is known the answer is easily obtained.

In summary, tests were run under these conditions and usually required from eight to thirty hours to complete depending on the number of changes required to be made to the independent variable under investigation.

EXPERIMENTAL RESULTS AND DISCUSSION

A: Batch Tests

In order to establish the operability of the thickener system previously described, several batch tests were done with both bentonite and silica. The suspensions were prepared in demineralized water (D.W.) at 0.5 per cent solids by weight. In all cases the suspension was vigorously mixed before settling was allowed to begin. A blank test (i.e. no voltage) was run concurrently with the cataphoretic assistance test to illustrate the difference in subsidence rates. The suspension characteristics are presented in Table 2.

Table 2: Suspension Characteristics for Batch Testing

<u>VARIABLE</u>	<u>SILICA</u>	<u>BENTONITE</u>
% Solids by Weight	0.5%	0.5%
Suspension Medium	600 cc D.W.	600 cc D.W.
Particle Mobility (Average)	6.0×10^{-4} cm ² / volt-sec	1.18×10^{-4} cm ² / volt-sec

The rates of subsidence were difficult to follow in the blank tests because a clear water-pulp interface never developed. This interface did develop in the systems with attached electrodes as would be expected since the imparted cataphoretic velocity would be the minimum settling velocity

of any particle. The tests with the silica flour revealed the sedimentation to be complete in approximately two hours while the blank test required a matter of days for complete sedimentation. This was also seen to be the case for the bentonite suspensions although the sedimentation in the cataphoretically assisted system was somewhat slower than for its silica counterpart as would be expected from the relative mobilities given in Table 2.

These qualitative results confirmed that such a system should work in a continuous thickener if the particle mobility, applied D.C. voltage gradient and the rate of overflow removal could be controlled. As a consequence of these results the continuous thickener system was designed and built and testing was begun.

B: Elucidation of the Operating Characteristics of the
Continuous Thickener With Cataphoretic Assistance

It was desirable to investigate how changes in certain independent operational variables would effect the clarification in the thickener. An experimental program was devised to look at these relationships. The program was as follows:

- i) The initial study to determine the effectiveness of cataphoretic assistance in a continuous thickener.
- ii) The effect of the voltage gradient and ultimately the power input on the overflow clarity.
- iii) The effect of the overflow flowrate on the overflow clarity.
- iv) The effect of the ionic strength of the slurry on the overflow clarity.
- v) The effect of electrode separation on overflow clarity.
- vi) The effect of the solids concentration in the feed on the overflow clarity.

The above tests were conducted following the 'one variable at a time' testing procedure and in all cases the other independent operational variables were held as constant as possible. Once the program had been set, it was necessary to determine which solid should be used to make the suspensions. The -400 mesh silica flour, a common constituent in ores or tailings, was chosen because it is clean, relatively inexpensive and because of its large mobility in water it will form a lyophilic sol.³⁴

It was confirmed* that this material receives no chemical (dispersant) treatment prior to packaging. It was also decided that, in the interests of practicality, Edmonton city tap water would be used in forming the suspension, as opposed to demineralized water. The decision was made because the tap water, due to its higher ionic content, more closely approximates the process water which may be found in such an application. A water analysis was obtained from the Power Plant Department and it is presented in Table 3. An arbitrary choice of 5 per cent solids by weight in the slurry was made, except for Test 6. Having decided on the test program and the slurry to be used testing was begun.

Preliminary Tests

i) Before proceeding with the actual clarification tests it was necessary to do some preliminary work. The first test was to investigate the mobility vs pH relationship for the silica colloid. The results of this test are presented in Figure 5.** There are two curves, labelled [1] and [2] drawn through the data points on Figure 5. Curve [1] is just a smooth type curve which attempts to relate mobility to pH as a non-linear function while curve [2] is the type which was illustrated in Figure 3 showing the plateau and reversal obtained in anionic

* Communication with Mr. J. Stukel, Process Eng., Ottawa Silica Company, Feb. 15, 1973

** All data and comments for the figures to be presented in this and the succeeding sections are contained in Appendix 2.

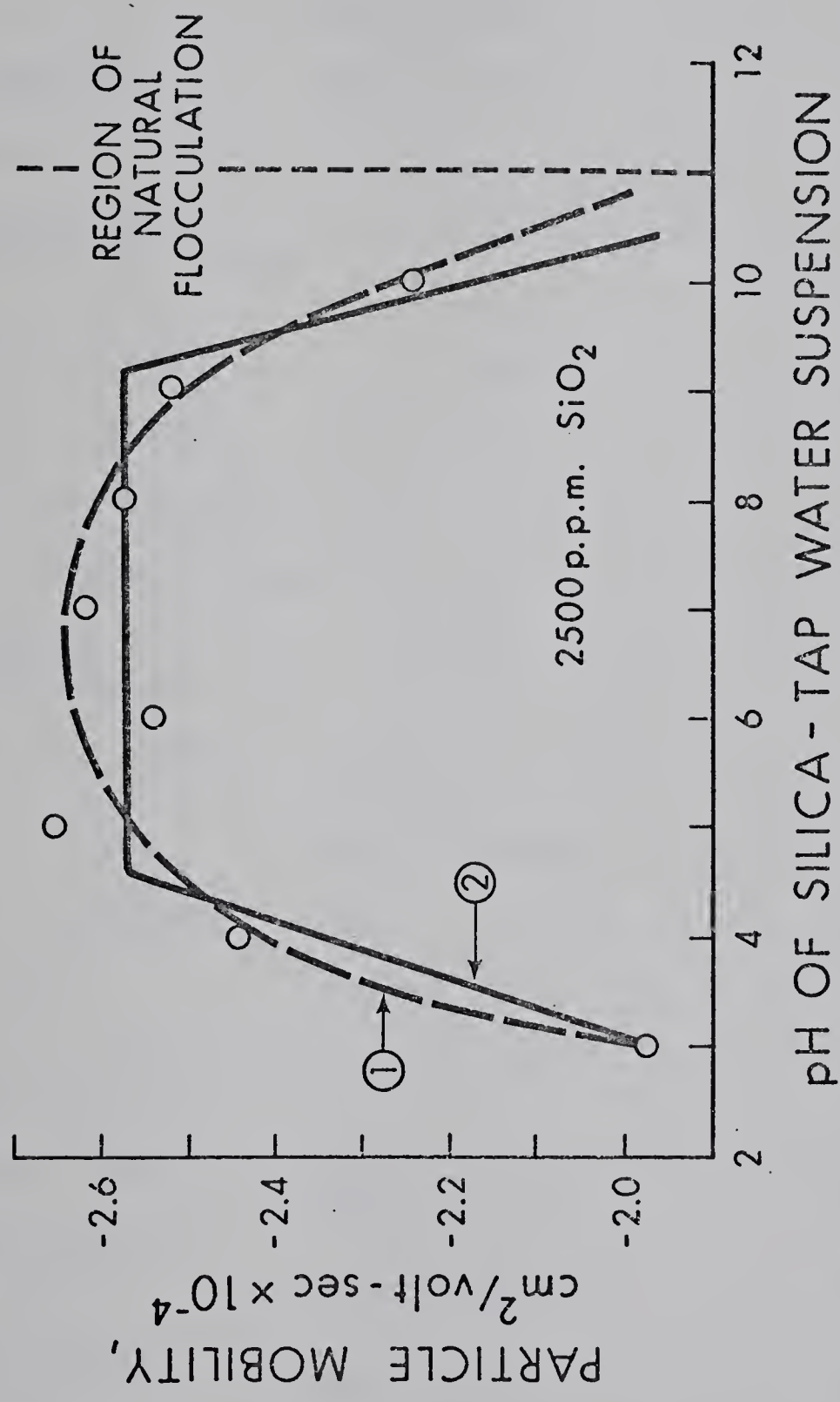


FIGURE 5: Cataphoretic Mobility of -400 Mesh Silica Flour Versus pH of a Silica-Tap Water Suspension

Table 3

The City of EdmontonPower Plant DepartmentAverage Water Analysis*

	<u>Summer Months</u> <u>May to Sept.</u> <u>(Inclusive)</u>		<u>Winter Months</u> <u>Oct. to April</u> <u>(Inclusive)</u>	
Dry Residue	29.	p.p.m.	15.	p.p.m.
Silica	-		-	
Aluminum and Ferric hydroxide	-		-	
Sodium chloride	5.	p.p.m.	5.	p.p.m.
Calcium sulphate	18.	"	12.	"
Magnesium sulphate	19.	"	24.	"
Calcium bicarbonate	54.	"	42.	"
Magnesium Bicarbonate	2.	"	4.	"
Sodium sulphate	10.	"	51.	"
Total solids	137.	p.p.m.	153.	p.p.m.
Total hardness	81.	"	75.	"
pH value	8.8	"	8.8	"
Bacteria count per c.c.	3.		0.	
Bacteria Coli	Nil		Nil	
Total cation conc.	28.	p.p.m.	38.	p.p.m.
Total anion conc.	80.	"	100.	"
[cation]/[anion]	0.35		0.38	

* Obtained October 12, 1973, with error estimated at ± 1 p.p.m. and peaking expected to occur in the middle of the stated time period.

dispersion curves. In the pH range from 5 to 9, within which many industrial operations run, there is little change in the mobility. A maximum deviation of ± 2.7 per cent based on the mathematically averaged mobility of $-2.59 \times 10^{-4} \text{ cm}^2/\text{volt-sec}$, is calculated. This would indicate that within this range, changes in pH will do little to alter the mobility the major concern being changes in the suspension conductivity which in turn will effect power input. A point of special interest is the region of natural flocculation observed when the pH was 11. (This was not observed at pH equals 1 or pH equals 2 which might be expected based on the Z.P.C. given earlier.) In preparing the samples for mobility measurements floccules were observed to form at pH equals 11 and pH equals 12 with those for the latter pH value appearing to be larger than in the case of the former. Since mobility measurements could not be made on these two samples their mobilities can only be estimated using Riddick's classification (18 pg. 2). The classification scheme is presented below.

<u>Suspension Stability Characteristics</u>	<u>Average Z.P.in Millivolts</u>
Maximum agglomeration and precipitation	0 to +3
Range of strong agglomeration and precipitation	+5 to -5
Threshold of agglomeration	-10 to -15
Threshold of delicate dispersion	-16 to -30

Moderate Stability	-31 to -40
Fairly Good Stability	-41 to -60
Very Good Stability	-61 to -80
Extremely Good Stability	-81 to - 100

Applying the Smoluchowski equation [1] to the mobility data from Figure 5 (this is the equation used by Riddick), calculations show the zeta potentials of the silica suspensions to range from -27.9 mv at pH equals 3 to -37.6 at a pH of 5.0, these being the extrema. Thus, under the above classification these suspensions should have moderate stability and they are observed to behave in this manner. It follows, from observations, on the samples with the pH greater than or equal to 11 that the zeta potentials of the colloid must be greater than -15 mv and because of the relative floccule size the zeta potential at a pH of 12 is greater than for pH equals 11. It would appear that this offers another method for clarifying silica suspensions although the reagent dosage and hence corrosive power of the slurry would probably warrant the use of something like AlCl_3 as its effectiveness in the flocculation of silica is quite high (Fig. 3). The shape of curve [2] is as expected from potential determining ions, in this case OH^- , under Riddick's bulk stress theory and the B.D.M. model of the double layer.

In summary minor pH fluctuations would not be expected

to change the particle mobility although some effect on power input may be observed.

ii) The second preliminary test was to determine the effect of silica concentration on the pH of the slurry. This test was done to ensure that large pH variations, depending on solids concentration, would not effect the system. The results showed that although initially, after mixing, there was a slight difference in the measured pH values for solids concentrations ranging from 0 per cent to 20 per cent by weight, there was very little difference after the 24 hour equilibration period (pH equals 8.0 for the slurries and pH equals 7.97 for tap water). The pH change from 8.9 as measured or 8.8 from Table 3 to 7.97 after standing for 24 hours is most probably due to carbon dioxide dissolution in the water. Under the conditions of sample preparation, CO_2 solubility is about 0.03 moles/litre and aqueous solutions can have an acid pH of 4.³⁵

The results of this test allow the conclusion that with the test procedure followed there will be no pH fluctuation in the system as a result of varying the solids concentration. The effect of concentration on mobility will be discussed under the results for Test vi.

iii) The third preliminary test was the determination of the size analysis of the silica flour. Two methods were used in this determination both the Warman Cyclosizer and the Hydrometer sedimentation analysis. Figure 6 shows the resulting curves and indicates good agreement between the

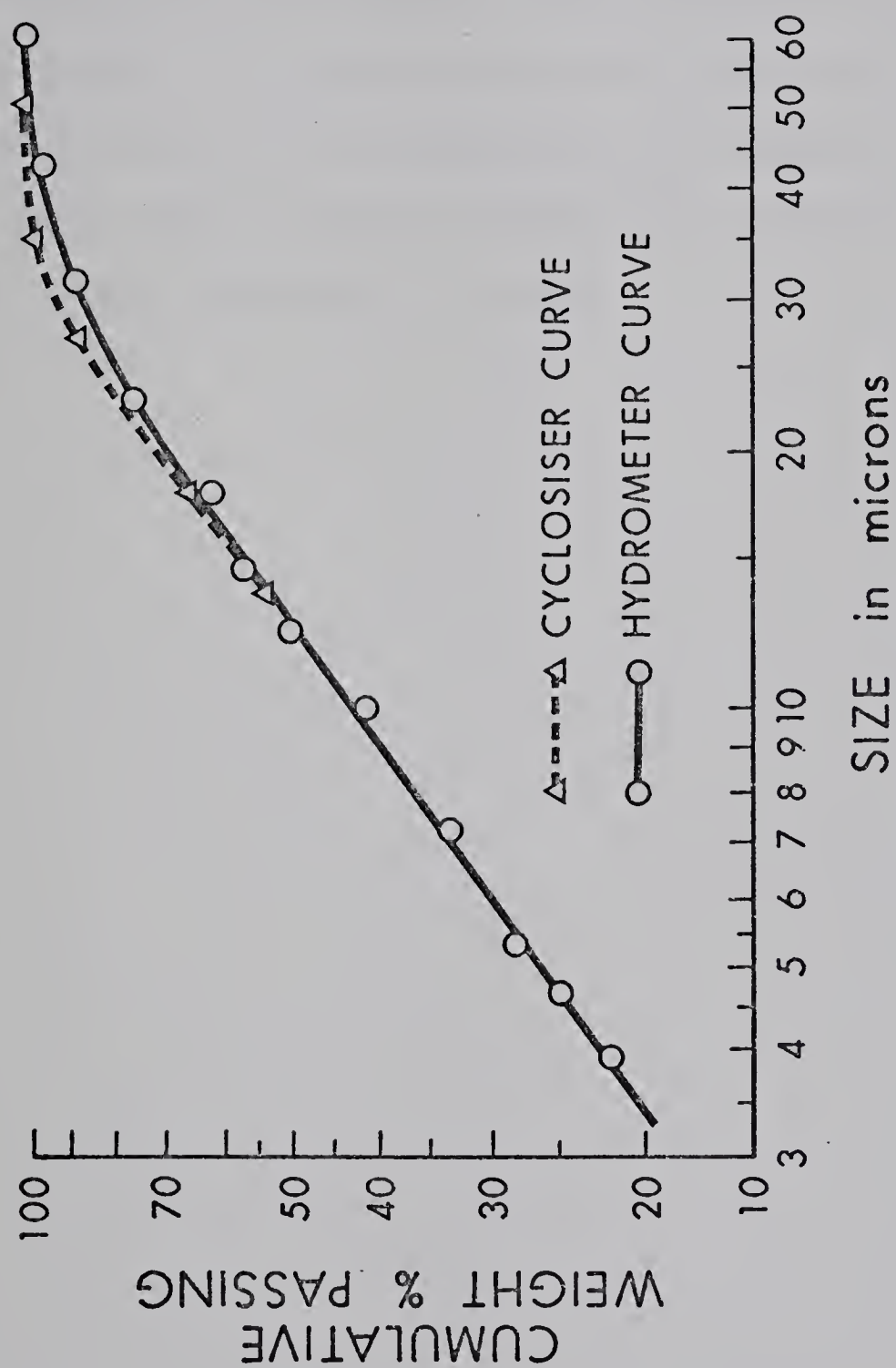


FIGURE 6: Size Analysis of -400 Mesh Silica Flour as Determined by Both Cyclosizer and Hydrometer Techniques

two methods.

iv) A relationship between water density as a function of temperature was required but rather than determine this experimentally the data was found in the literature, and the curve is presented in Figure 7. This relationship is necessary to solve equation [4] and determine the solids content of a thickener discharge.

With the preliminary tests complete testing was begun in the continuous system.

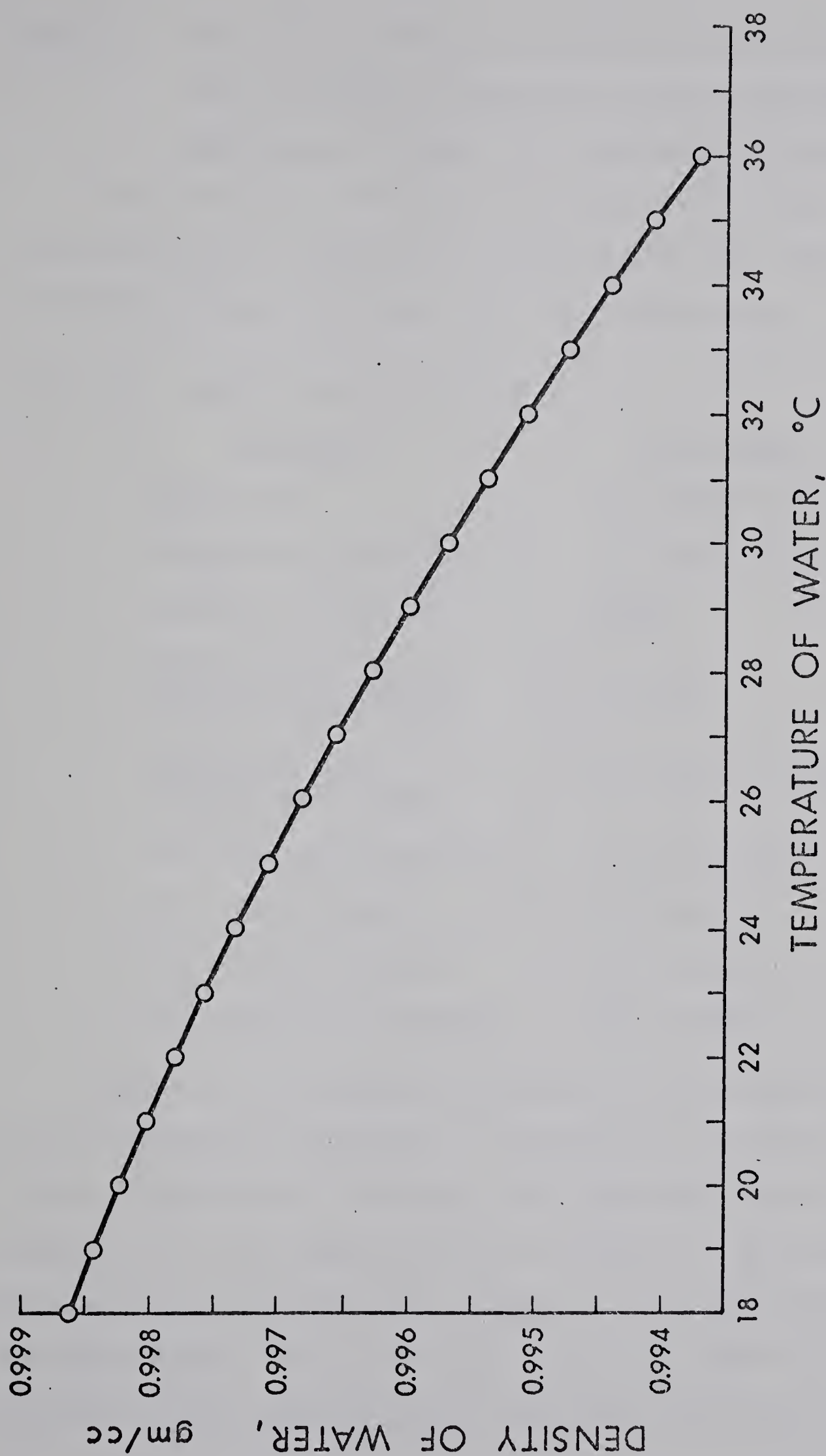


FIGURE 7: The Density of Water as a Function of Temperature (Extracted from Table 290, "Smithsonian Physical Table", 9th Rev. Ed., Washington D.C. 1954)

Test # 1 - The Initial Study to Determine the Effectiveness
of Cataphoretic Assistance to the Gravitational
Settling of Silica in a Continuous Thickener

The results of this test were most gratifying. They are presented in Figures 8, 9, and 10 with the other pertinent information about the test being given in Table 4.

Table 4: Conditions for Test # 1

<u>VARIABLE</u>	<u>TEST VALUE</u>
Slurry mix	5% -400 m SiO_2 in tap water
Electrode Separation	14 inch/ 35.6 cm
Chemicals Added	None
Depth of First Feed Well Discharge Below Cathode	1 inch
Thickener Pulp Temperature Range	21.1 $^{\circ}\text{C}$ to 23.8 $^{\circ}\text{C}$
Ave. Voltage Gradient	3.4 volt/cm
Ave. Power Input	250 watts
Ave. Feed Flowrate	820 cc/min
Ave. Overflow Flowrate	690 cc/min

Figure 8 is included to show the effectiveness of the refrigeration equipment in maintaining a constant feed slurry temperature. Although the temperature does rise slightly when the power to the electrodes is switched on, the equipment operates well enough to suit the purposes of these tests. This particular plot was done for several of the tests to ensure that the performance of

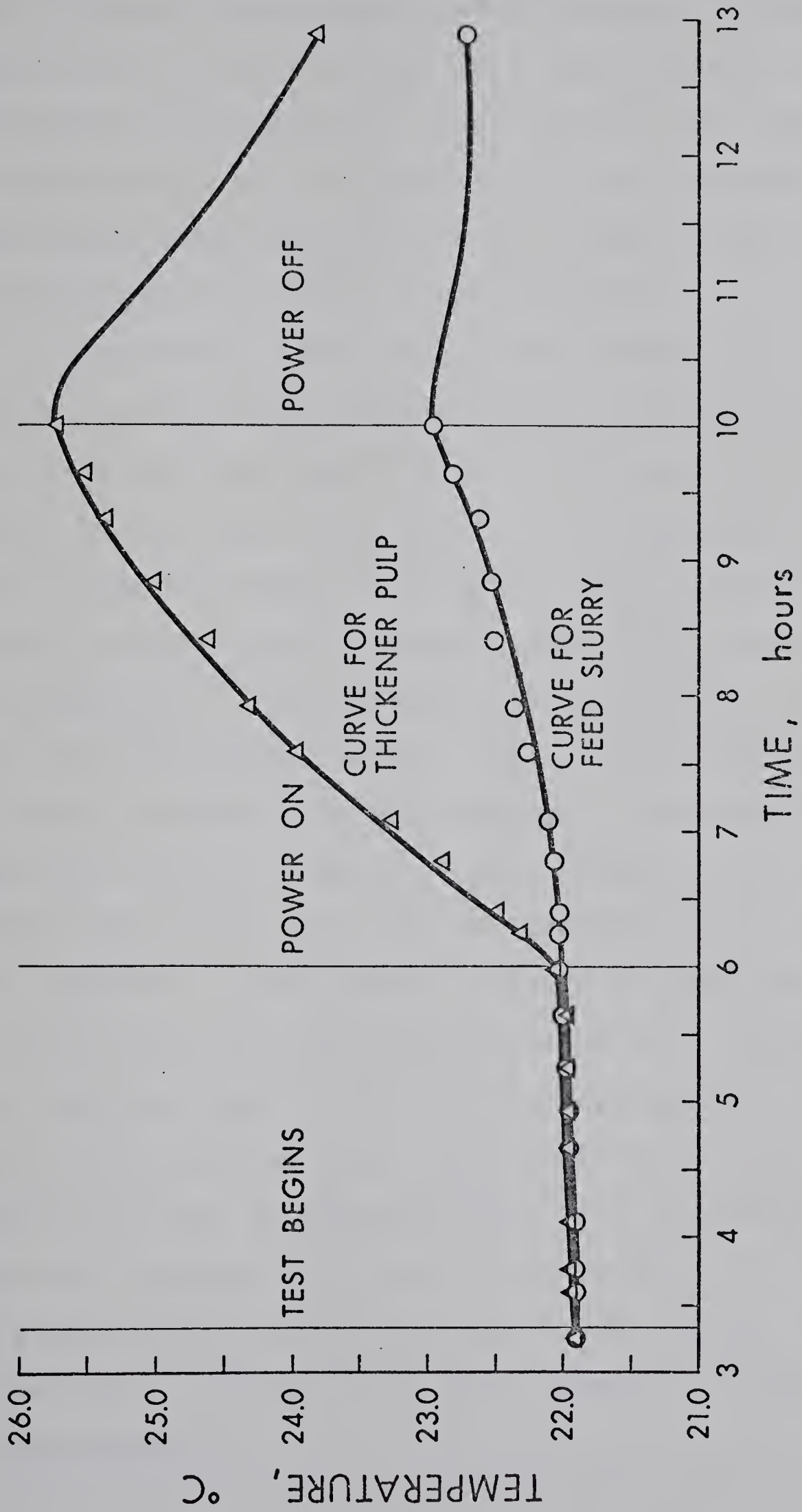


FIGURE 8: Temperature Profiles for Test 1

the refrigeration equipment did not change. This was found to be true and in later tests monitoring of the feed slurry temperature was discontinued. The temperature of the thickener pulp was monitored in all cases to enable water densities to be found in the calculation of the solids content of the underflow (S_u).

The contents of table 4 plus the information on figures 9 and 10 allow a mass balance to be performed around the thickener-clarifier to calculate the solids content in the feed slurry (S_f). It was expected that at steady state the value of S_f would differ, in some degree, from the quoted value for the original slurry mix of 5 per cent solids. Unfortunately, in this test, it was found that the torsion balance used in S_u determinations was faulty, resulting in high readings. This error was found only after the power had been turned on and was probably the result of a lack of lubricant in the beam shaft sleeves. In any event, reliable readings were obtained after the power had been turned on. Calculations, using average values for S_o and S_u , indicated the value of S_f to be 9.2 per cent under these conditions. Since complete data for S_f determinations were not available in this test the analysis of variations in S_f will be left to the discussion of results for test 2. The trends evident on the curve in figure 9 are real, however, and require an explanation.

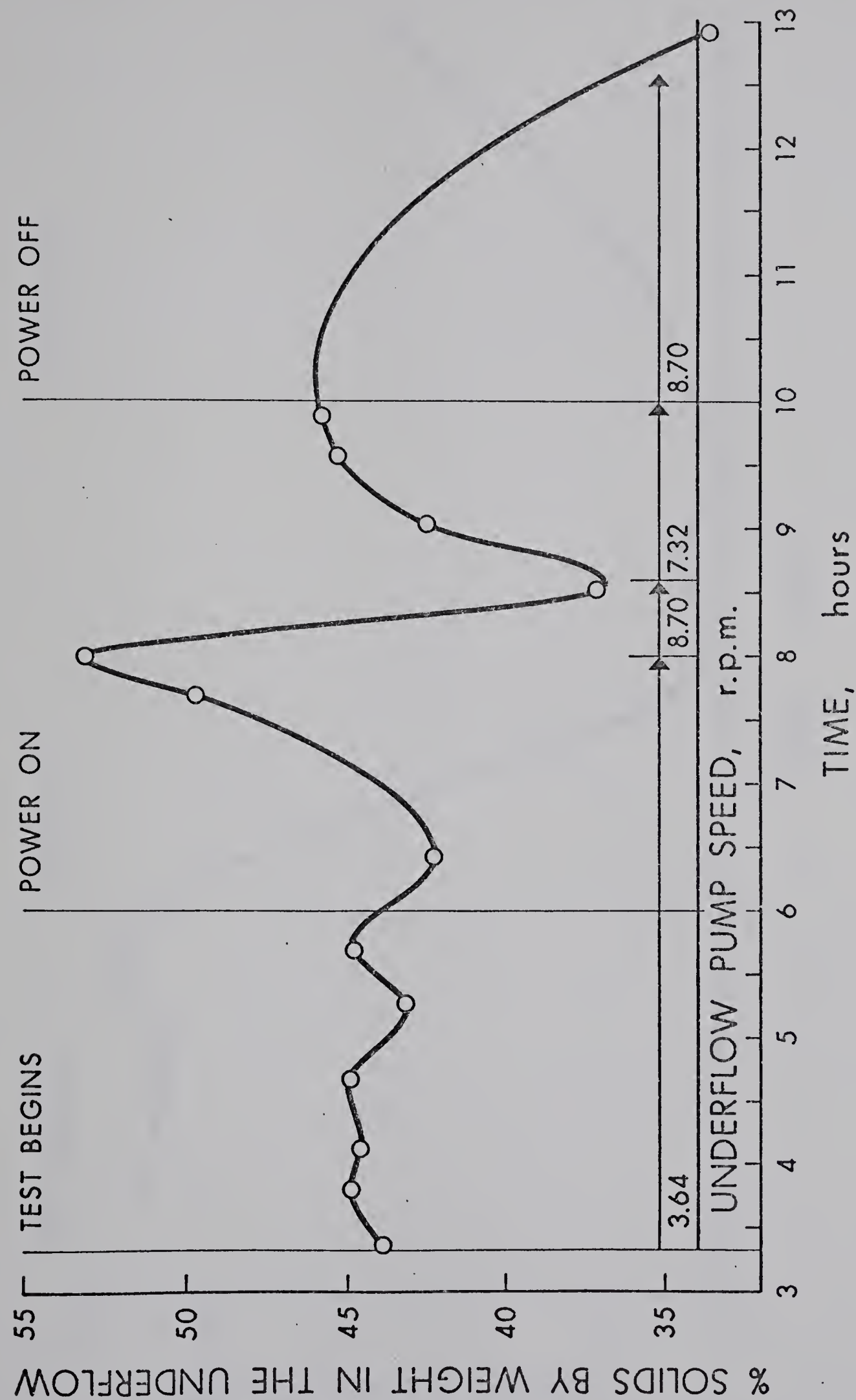


FIGURE 9: Underflow Solids Concentration Versus Time for Test 1

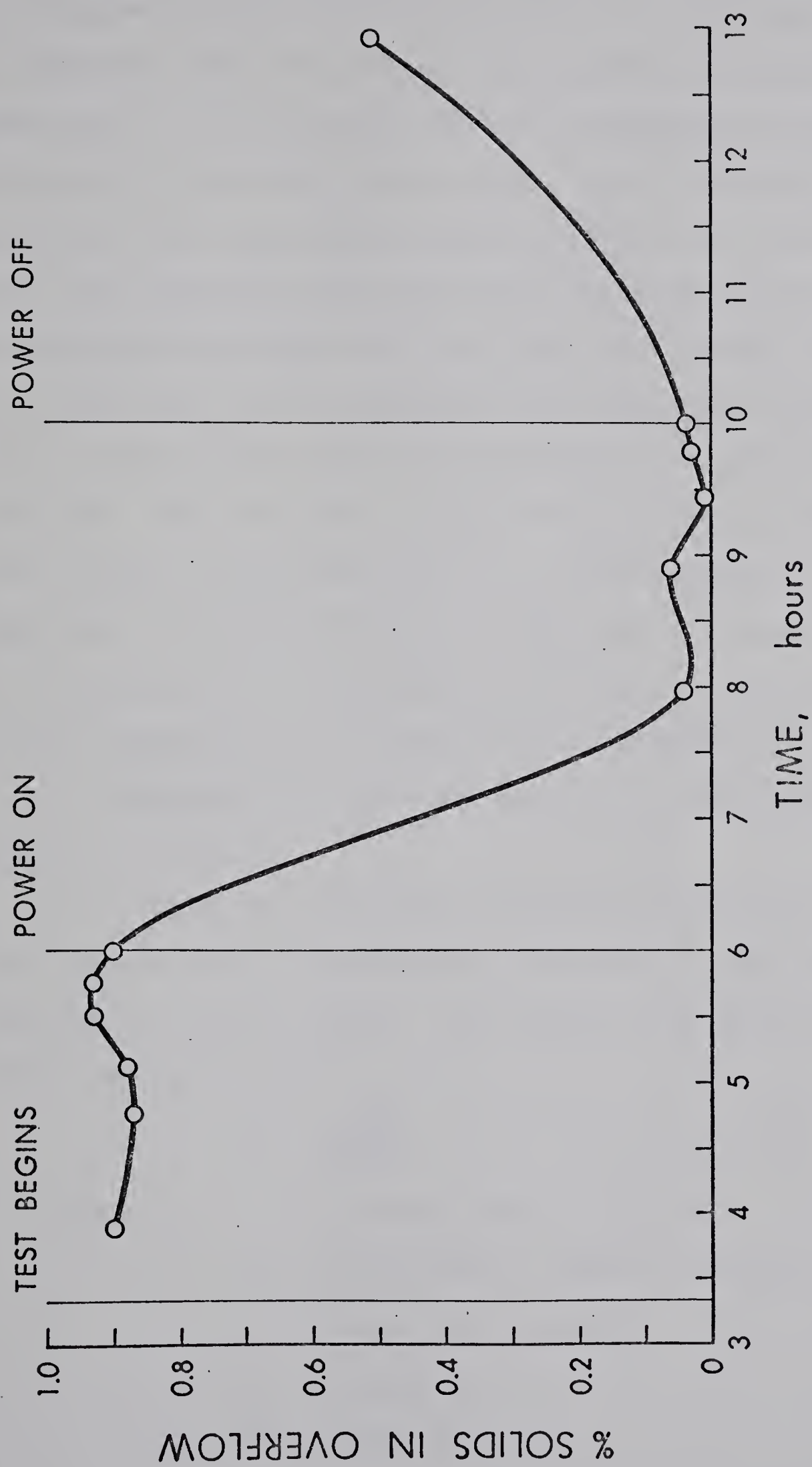


FIGURE 10: Overflow Clarity Versus Time for Test 1

Figure 9 shows how the S_u varies as a function of time both with and without cataphoretic assistance. When there is no assistance the S_u is reasonably constant at something less than 43 per cent. When the power is turned on, the curve then climbs to 53 per cent. (At this point the underflow pump speed was increased to lower S_u , because previous experience had shown that values in excess of 55 per cent led to plugging in the underflow discharge line.) The reverse trend is illustrated when the power is shut off. This increase in the solids content of the underflow is due, for the most part, to electro-osmosis. The phenomenon of electro-osmosis is the reverse process of particle deposition by cataphoresis, and, it causes a gradual dewatering of the deposit and therefore an increase, in S_u . Mathematically this process can be described by equation [5] below.

For simplicity, consider a single capillary tube, (the deposit may be considered as bundles of such tubes connected in diverse ways). The formula for the electro-osmotic velocity is:¹³

$$V = \frac{Ee\xi}{4\pi n} \dots\dots\dots [5]$$

where

- V = electro-osmotic velocity
- E = magnitude of applied electric field
- e = dielectric constant
- n = viscosity
- ξ = zeta potential

Thus when the power is turned on and E established, the electro-osmotic velocity is proportional to the zeta potential in a given medium. The direction of migration of the water is upwards since water is positively charged with respect to the silica ([34] A III, pg. 58). Removal of the water and cations from the deposit serves to increase its resistance. Ohm's law, equation [6] indicates that current must increase to give the same voltage gradient across the floc zone and thereby increase total power input.

$$V = IR \text{[6]}$$

where V = voltage
 I = current in amps
 R = resistance in ohms

It may or may not be economically advantageous to increase the underflow withdrawal rate to hold the resistance at a lower value and hence minimize power input.

Figure 10 indicates the effect on S_o when power is applied. Without power the average S_o equals 0.9 per cent while with power this value is reduced to 0.04 per cent. This represents a clarification of $(0.9 - 0.04)/(0.9) * 100$ per cent equals 96 per cent. Figure 8 showed a temperature rise in the thickener when the power was on due to resistance heat losses, (I^2R) . This temperature increase is a desirable side effect of the cataphoretic assistance, since it tends to increase the settling velocity. Unfortunately this effect is only beneficial to the larger particles which would most probably settle any-

way but the probability is increased as a result of this effect. The fact that the temperature increase is unimportant in the clarification observed, can be illustrated in a simple calculation using Stokes' law, equation [7].

$$V_t = \frac{D^2 g (P_s - P_w)}{18n} \dots\dots\dots [7]$$

where V_t = the terminal settling velocity
 D = the equivalent spherical diameter of the particle.
 g = the gravitational constant
 P_s = the solid density in the liquid
 P_w = the liquid density
 n = the liquid viscosity

This calculation is meant strictly as an illustration and the applicability of Stokes' law is dubious since the settling velocity is a function of solids concentration according to Coe and Clevenger. Thus, Stokes' law will predict the maximum settling velocity for these particles and consequently the maximum contribution that temperature will make to the overall sedimentation rate.

Most of the tests conducted have a temperature range of 20°C to 26°C, as shown on Figure 8. It was determined, using Fisher Sub Sieve Size Analysis, that the average equivalent spherical particle diameter in the overflow, without power, was 1.3 microns. Table 5 presents the data needed to solve equation [7] at the two temperatures with the solutions and the velocity ratios. (Note: The Einstein

viscosity correction formula for dilute suspensions, has not been applied since it will cancel out in the ratio and makes negligible difference in the absolute value of V_t .) Further, the average particle mobility for this suspension was found to be -2.56×10^{-4} cm/volt-sec from Figure 5. The voltage gradient was 3.35 volts/cm which means an imparted cataphoretic velocity of 8.57×10^{-4} cm/sec.

Table 5: Solution to Stokes' Equation for Sample Calculation

<u>TEMPERATURE</u>	<u>20°C</u>	<u>26°C</u>
D	1.3×10^{-4} cm	1.3×10^{-4} cm
g	980 cm/sec ²	980 cm/sec ²
Ps	2.59 gm/cc	2.59 gm/cc
n	$1 \times 10^{-2} \frac{\text{gm}}{\text{cm} \cdot \text{sec}}$	$0.877 \times 10^{-2} \frac{\text{gm}}{\text{cm} \cdot \text{sec}}$
Pw	0.99823 gm/cc	0.99681 gm/cc
Vt	1.46×10^{-4} cm/sec	1.68×10^{-4} cm/sec
Ratio	$V_t (26^\circ\text{C}) / V_t (20^\circ\text{C})$	1.15

Table 5 shows a 15 per cent increase in the settling velocity with the temperature increase but, dividing this increase with the total settling velocity, including the cataphoretic velocity, the net contribution is only 2.5 per cent. Since this is a maximum value, it is safe to assume that temperature increase plays only a very minor role in the clarification of the overflow, when the power is on.

The illustrative calculation shows that the cataphoretic assistance in the thickener, under the test conditions, is an effective means of clarifying the overflow.

Test # 2 - The Effect of the Voltage Gradient on Overflow Clarity

This test was designed to determine the effect of the applied D.C. voltage gradient and ultimately the power input, on the overflow clarity. The results are presented in Figures 11, 12, and 13 as well as in Table 6. The procedure followed was to begin without power and when steady state was reached full power was applied (according to the source limits), thereafter power reductions were made by appropriately adjusting the applied voltage until the test was complete.

Table 6: Conditions for Test # 2

<u>VARIABLE</u>	<u>TEST VALUE</u>
Slurry	5% -400 M in tap water
Electrode Separation	14 inch/35.6 cm
Chemicals Added	None
Depth of First Feed Well Discharge Port Below Cathode	1 inch
Thickener Pulp Temperature Range	22.0 ⁰ C to 26.0 ⁰ C
Ave. Volt Gradient	Under Test
Ave. Power Input	Under Test
Ave. Feed Flowrate	900 cc/min
Ave. Overflow Flowrate	760 cc/min

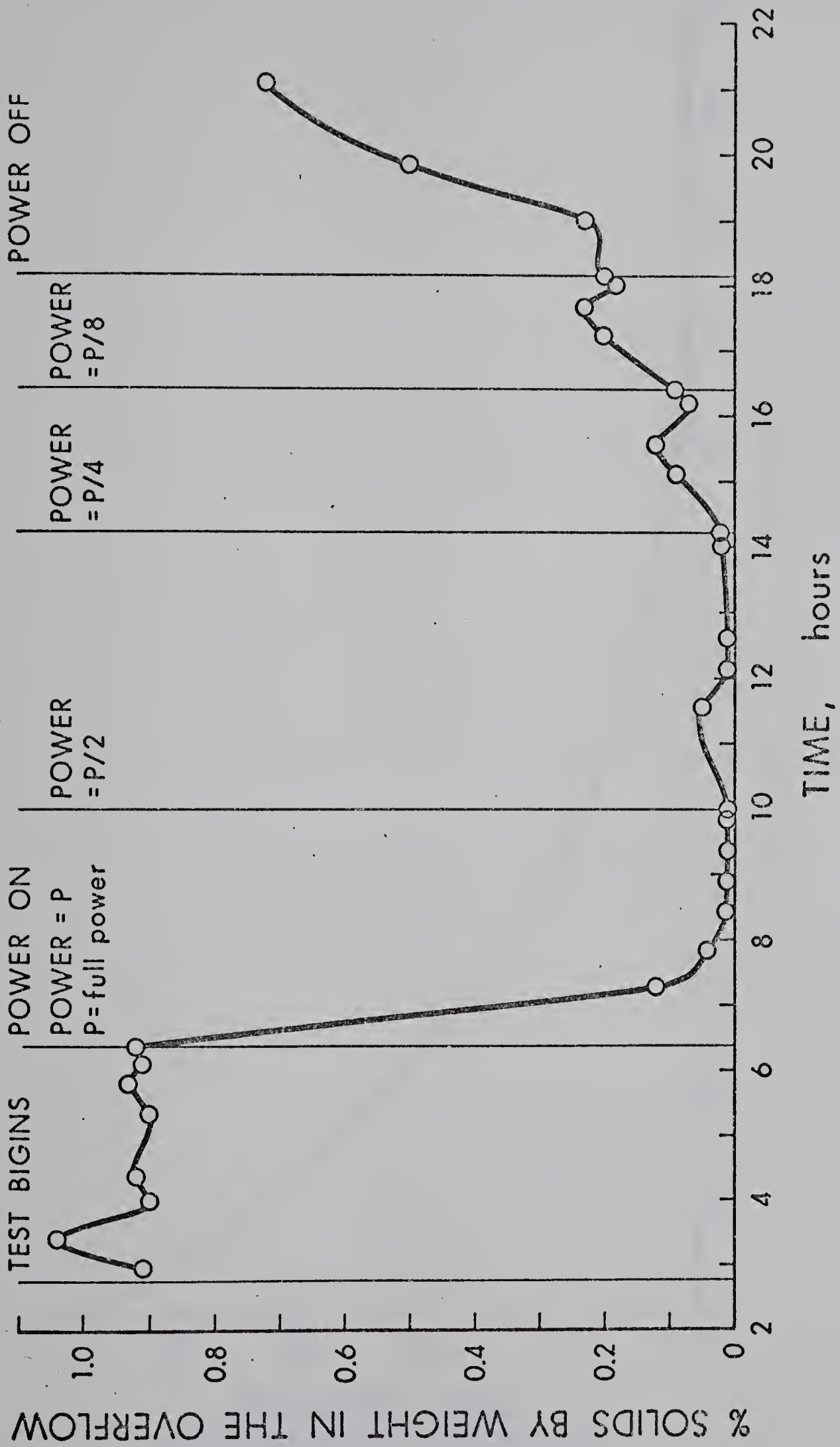


FIGURE 11: Overflow Clarity Versus Time for Test 2

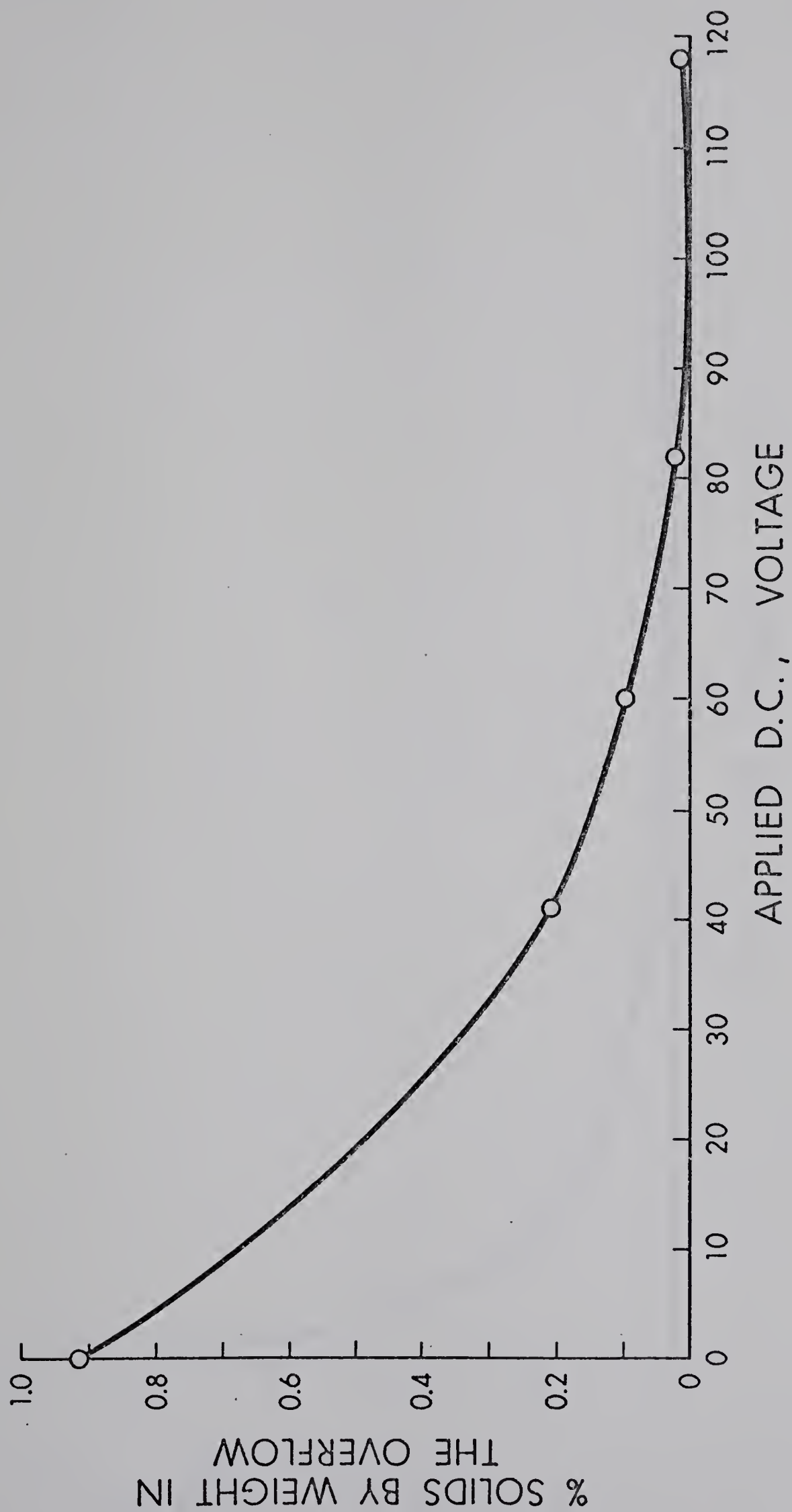


FIGURE 12: Overflow Clarity as a Function of Applied Voltage for Test 2

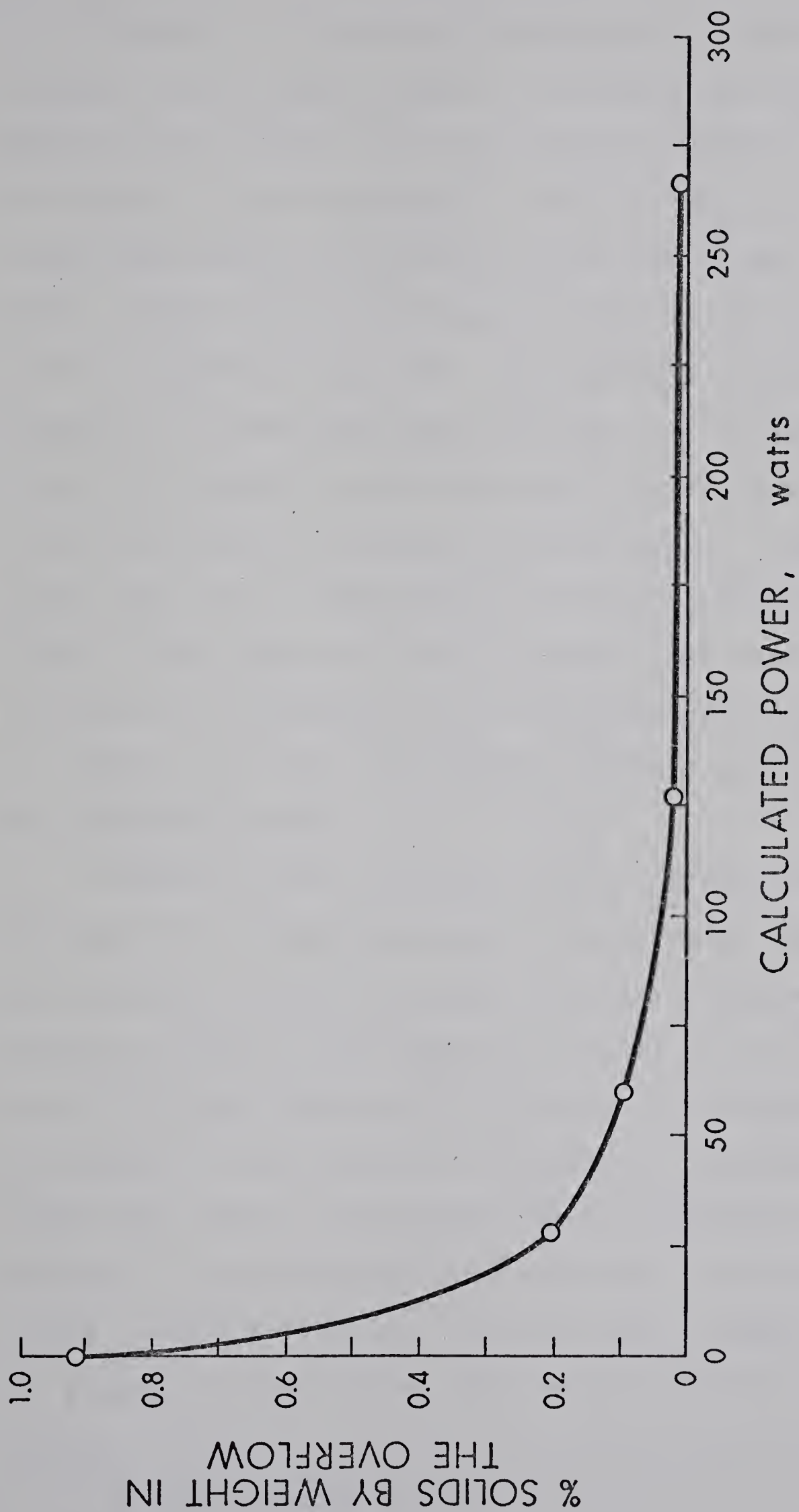


FIGURE 13: Overflow Clarity as a Function of Power Input for Test 2

Figure 11 illustrates the response of the overflow clarity to the applied power. It should be noted that the points which lie on the lines indicating power changes, in Figure 11, are averages of the last three (or four where applicable) S_o readings before the change was made. These are the ordinate values used in the construction of Figures 12 and 13. The important feature of Figure 11 is the curve when the power is shut off. The curve is climbing toward the steady state value of S_o that was initially observed, without power. This indicates that there are no flocculation effects in this system. Thus, if any agglomeration is present, the shear forces provided by the pumping and mixing machinery are enough to destroy the flocs and restore particle singularity to the thickener feed.

Figures 12 and 13 illustrate the relationship between S_o and both voltage and power* respectively. The curves are somewhat similar in shape, exhibiting maxima when the abscissa value is zero and then falling in an exponential manner to some limiting S_o as the abscissa value increases. The shape of the curves is of particular economic interest since they show a point beyond which negligible increase in clarity is realized for large increases in power or voltage. (This is most evident for the S_o vs power input curve.) As an example, if the system were run at 82 volts (127 watts)

* Power is calculated by multiplying the applied voltage by the measured current, i.e. $P = VI$.

an increase to 119 volts (266 watts) improves the clarity by 42 per cent but the power increases by 110 per cent. It must also be remembered that the clarity at 82 volts is quite good such that a 42 per cent improvement does not represent much of a change. These curves or at least that which relates S_o to power are important in determining, in part, the economic viability of such an application as well as providing operating limits.

It was mentioned that the curves had a similar shape.

The boundary conditions are: $Y = Y_{\max}$ when $X = 0$

and: $Y = Y_{\min}$ as $X \rightarrow \infty$

The general equation, [8], for the curve is:

$$Y = Y_{\max} e^{-kx} \dots\dots\dots [8]$$

when, as in this case $Y_{\min} = 0$ as $X \rightarrow \infty$. Two variable linear regression was done for both data sets and the results given in Table 7.

Table 7: Regression of Equation [8] for S_o vs Both Power and Voltage

<u>VARIABLE VALUE</u>	<u>S_o vs VOLTAGE</u>	<u>S_o vs POWER</u>
Y max	0.91%	0.91%
k	0.04	0.015
Y intercept (= 0 theoretically)	-0.021	-0.951
Correlation Coefficient*	-0.98	-0.902
Upper and Lower k limits**	-0.03 -0.05	-0.002 -0.029

* A correlation coefficient of ± 1.0 indicates a perfect fit.

** Calculated from a two sided t statistic test at 95% confidence limits.

Table 7 illustrates that equation [8] can be used to predict the S_o response to voltage to a good approximation while the correlation is not as good for Figure 13. The reason for this observation is that although voltage can be held constant, the system resistance and hence current and power change as some function of voltage. (e.g. electroosmotic effect.) These changes are not large enough to prevent the system from reaching steady state but they result in the use of average power values for curve construction which results in the larger deviation when attempting to fit the power data to equation [8].

Another interesting feature of Figure 12, is that most of the clarification is done over the initial voltage range. Since, according to Smolochowski's equation [1], mobility is directly proportional to the voltage gradient, all other things being equal, it would appear that the majority of particles are deposited when the net upward velocity is a minimum. That is, if small voltages show marked results, the particles must have a negligible upward velocity. The very fine particles act as part of the fluid and can only be removed by large applied voltage which would account for the limiting value evidenced in Figures 12 and 13. A detailed discussion of this observation is beyond the scope of this work.

It was mentioned in the discussion of results for test 1, that the value of S_f was expected to differ from the 5 per cent value of the original mix. Using data from

table 6 and figure 11 along with S_u data contained in appendix 2 for figure 11, mass balances were performed. These balances were done at the differing power levels. In the first case, with no power input, the value of S_f was found to be 8.1 per cent. This simply means that of the original slurry mix, at steady state operation, a greater percentage of liquid is retained in the thickener-clarifier, relative to the solids. The effect of power on S_f is as follows: For the power inputs quoted on figure 11 the corresponding values of S_f in per cent are 8.1, 9.1, 8.4, and 8.0. There was, of course, some error associated with the measurement of the variables used in the mass balance calculations never the less a trend is evident. That is, as power increases so does the value of S_f , all other independent operational variables being constant. This can be explained by applying the theory of electro-osmosis in the anode deposit, as discussed earlier. The rate of electro-osmosis is directly proportional to the applied electric field, also, the value of S_u is proportional to the rate of electro-osmosis as was evidenced earlier and hence S_u is proportional to the applied electric field. The result, is that as power input increases the value of S_u increases making it easier for the rakes to remove solids from the anode. This happens because the deposit becomes less inclined to fluid flow and can be more easily controlled and directed to the discharge by the rakes. The increase of S_f , although inadvertent, makes

clarification increasingly difficult as will be discussed in test 6. This serves to reduce the clarification efficiency, to some degree, as power input increases. The magnitude of the effect cannot be determined as it is a complex function of the independent operational variables but it is to be kept in mind that if anything, the clarification possible with cataphoretic assistance could be slightly better than that observed in these tests.

In summary, the overflow clarity responds to applied voltage in a manner as mathematically described by equation [8], and Figure 12. To a lesser extent, the overflow clarity responds to power input also according to equation [8] but it is a more complex function because of time resistance changes. Figure 13, or one similar to it, is necessary for the economic evaluation of such an application for operating purposes.

Test # 3 - The Effect of Overflow Flowrate on Overflow Clarity

This test was designed to determine the effect of increasing the overflow flowrate (Q_o) on the overflow clarity. The results are presented in Figure 14 and Table 8. The procedure followed was to bring the system to steady state then turn the power on, and once steady state had again been reached the feed rate (Q_f) was increased, at constant underflow flowrate (Q_u), to increase Q_o . This increase in Q_f was done three times until the data for Figure 14 had been obtained.

Table 8: Conditions for Test # 3

<u>VARIABLE</u>	<u>TEST VALUE</u>
Slurry	5% -400 M in tap water
Electrode Separation	14 inch / 35.6 cm
Chemicals Added	None
Depth of First Feed Well Port Below Cathode	1 inch
Thick. Pulp Temp. Range	21.3 ⁰ C to 27.3 ⁰ C
Ave. Volt Gradient	3.9 volts/cm
Ave. Power Input	246 watts
Ave. Feed Flowrate	Under Test
Ave. Overflow Flowrate	Under Test

Figure 14 indicates, with a straight line parallel to the abscissa, that without power and Q_o equals 820 cc per min the S_o equals 0.9 per cent. When the power was

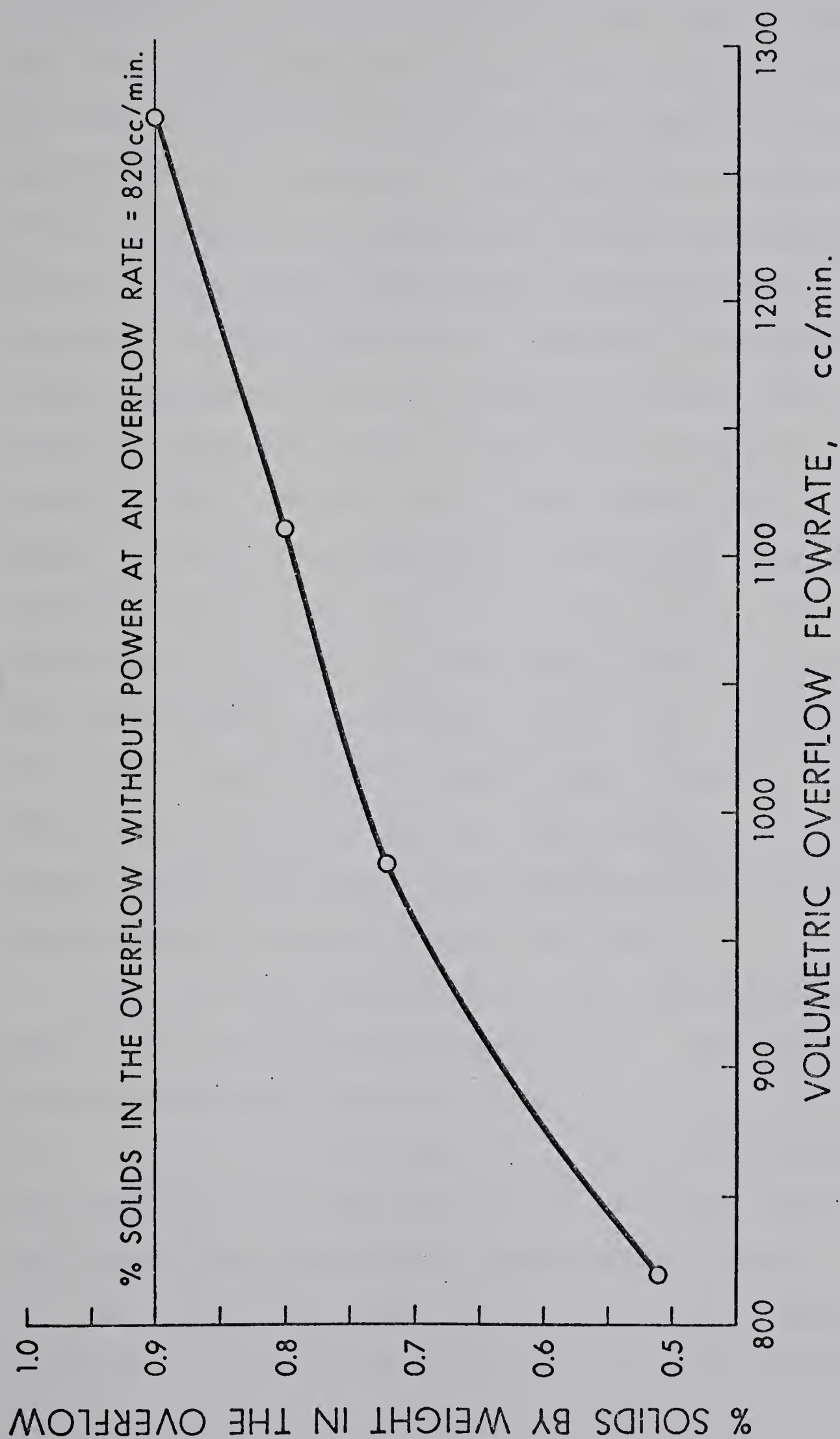


FIGURE 14: Overflow Clarity as a Function of Volumetric Overflow Flowrate for Test 3

turned on this value dropped to 0.51 per cent at the same Q_0 . (The reason why this result does not match that of Test No. 1, in terms of clarification, will be discussed in Test No. 4.) Increases in the feed rate and hence overflow rate served to increase both S_o and S_u , although the latter is not shown, since Q_u was constant this was to be expected. Further, the results show that the overflow flow-rate, with power, can be increased to 155 per cent of its original value (Q_f to 146 per cent of its original value) without power, and the same clarity can be achieved in both cases. This is not a favorable relationship though, because increasing Q_0 by 155 per cent increases S_o by 176 per cent, which does not give a 1:1 correspondence which would be the minimum desired in a practical application. In any event, this result shows that as long as the thickener is running far enough below the feed rate which induces sliming, surges in the feed rate can be handled by the cataphoretic system without drastic loss of efficiency.

Again, as for Test No. 2, two variable regression was done on the data, when the power was on. The data was plotted according to equation [9].

$$y = mx + b \dots\dots\dots[9]$$

The results of the regression on S_o vs Q_0 was equation [9a] which had a correlation coefficient of 0.98.

$$S_o = (8.5 \times 10^{-4}) Q_0 - 0.15 \dots\dots\dots[9a]$$

Plotting the data for Q_f serves only to shift the data.

to larger x co-ordinates resulting in the same equation only with y intercept now equal to -0.28 .

The effect of varying feed flowrate on S_f gave some peculiar results in this test. Combining the data from appendix 2 for figure 14 with that of table no. 8, mass balances were calculated to allow calculation of S_f values. The results were that without power and Q_f equal to 970 cc/min the S_f value was 8.6 per cent. Under these conditions with the power on S_f equalled 9.2 per cent as would be expected considering the electrosmotic effect on S_u and indirectly S_f . Increasing Q_o , with the power on, to 1130 cc/min or greater served only to drop the S_f value to 8.1 per cent where it remained relatively constant. A gradual decrease in S_f from 9.2 per cent may have been expected as Q_o was increased from 970 cc/min. It is difficult to speculate on the mechanism whereby these effects on S_f are observed. Suffice to say that it will make the curve for figure 14 depart from linearity a little more by lowering the ordinate S_o value for the left most point.

In summary, there is a linear response of overflow clarity to overflow flowrate and although the response is unfavourable, it does not indicate drastic changes in S_o with surging in the thickener feed.

Test # 4 - The Effect of Ionic Strength on Overflow Clarity

This test proved to be of great practical importance in the tests with silica as the suspended colloid. Before considering the actual clarification test in the thickener some other results, directly related to this test, are discussed. As was mentioned earlier, tap water was used to slurry the silica both because of its availability and its similarity to industrial process water. The clarification testing in the thickener commenced in mid June of 1973, and as testing proceeded through to September of 1973, the results of the tests, under the conditions which Test no. 1 was run, became increasingly poorer. (This was pointed out in the discussion of Test no. 3.) Finally, on an aborted test run on September 4th, 1973, under these conditions, the clarification was only 13.5 per cent as opposed to the 96 per cent obtained in Test no. 1. The reason for these observations is easily explicable with the use of Table 3. From Table 3 it is shown that in the summer there is a build up of divalent cations in the water while in the winter it is the monovalent cation concentration which increases. Table 9, which results from calculations performed on the entries in Table 3, illustrates these respective increases.

Table 9: Salt Conc. Buildup as a Function of Season

<u>SALT TYPE</u> <u>(cation)</u>	<u>SUMMER</u> <u>CONCENTRATION</u>	<u>WINTER</u> <u>CONCENTRATION</u>
Divalent	22.9 ppm	19.4 ppm
Monovalent	5.2 ppm	18.3 ppm
% increase	18%	-
lower value	-	252.%

Thus, in the summer, the absence of $\text{SO}_4^{=}$ (specifically Na_2SO_4) and the presence of Ca^{++} and Mg^{++} tend to lower the zeta potential both by reducing the surface potential (absence of $\text{SO}_4^{=}$) and shielding this potential more effectively (presence of divalent cations). In the winter the reverse effect holds, causing an increase in zeta potential. These effects were discussed in the electrical double layer theory. It is of note that although shielding is an important consideration for suspensions of minerals like SiO_2 it is much less pronounced in clay systems.³⁶ Unfortunately, in these tests, the flocculation effect in the summer was not strong enough to be beneficial to the clarification, since, although it lowered the zeta potential and hence the cataphoretic mobility, the particles were able to remain in colloidal suspension.

With these results it was decided to run future tests using demineralized water to slurry the silica and sodium chloride to adjust the ionic content of the suspension. Before proceeding with the actual clarification test in

the thickener, two preliminary tests were done. First, a Talmadge and Fitch test ²⁸ was set up for both 5 per cent silica in demineralized water and for the same mixture at 175 ppm NaCl. This was done to establish whether the subsidence rate of the colloidal particles would be affected by the salt. There was no observable increase in the settling rate in the salt test, consequently, any related observations in the clarification tests are due to changes in either particle zeta potential and/or liquid conductivity and not flocculation. Secondly, a plot was constructed to show the relationship between mobility and Na^+ concentration for the NaCl electrolyte. This curve is presented in Figure 15.

The curve for the 5 per cent silica slurry has the shape expected, from the double layer theory. The important feature of this curve is that above a sodium ion concentration of about 24 ppm, the mobility of the colloids changes very little, up to the limit of the plot (65 ppm).

With these preliminary tests completed the clarification test in the thickener was undertaken. The procedure was as follows: the power source was turned on when the tank was filling. After steady state had been reached a known amount of NaCl was added to the system in the feed tank and using both S_u and changes in meter readings, the system was followed to steady state. This procedure was repeated until the results for sodium ion concentrations

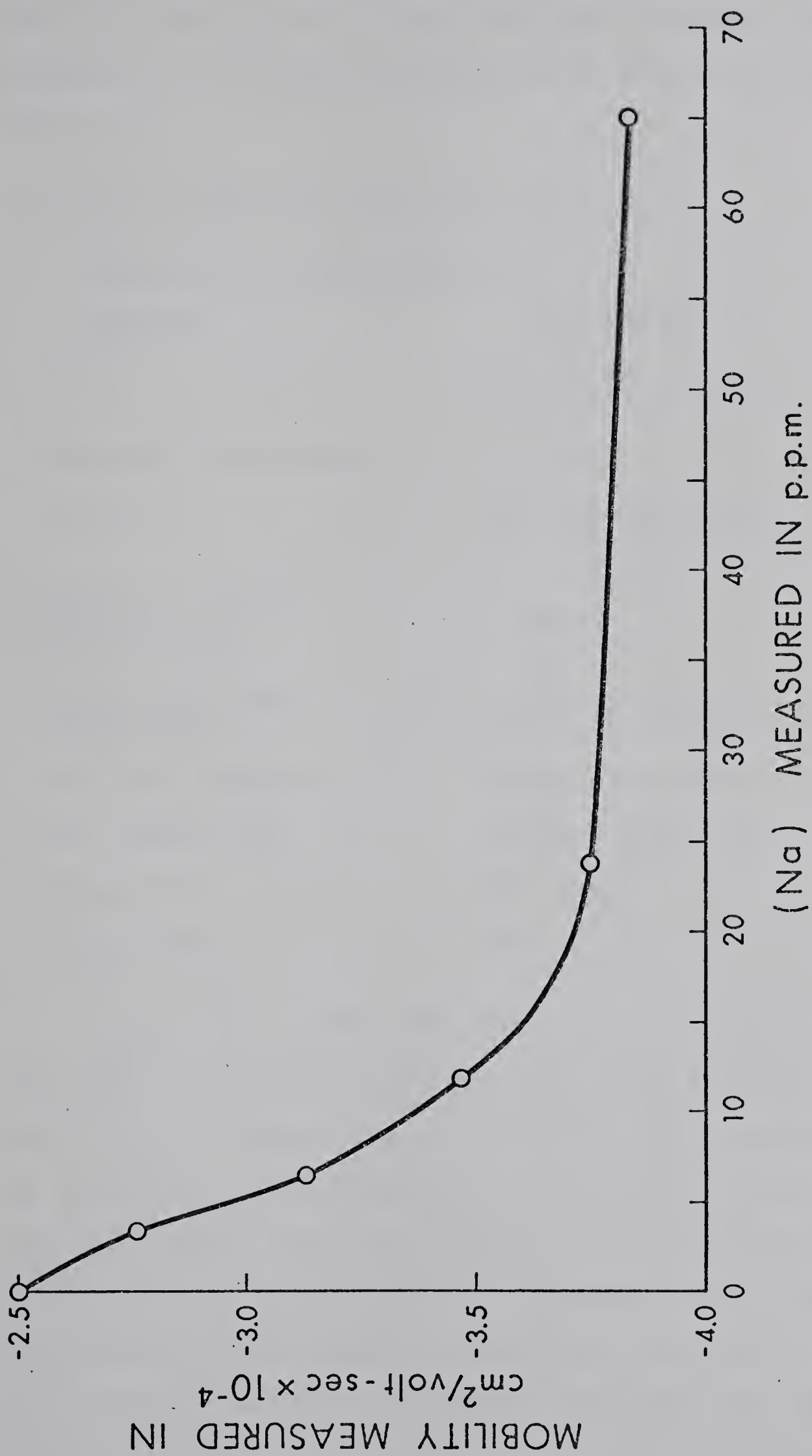


FIGURE 15: Silica Particle Mobility as a Function of Sodium (from Sodium Chloride) Concentration

of 0, 19, 29, 48, and 66 ppm had been obtained. The results of this test are presented in Figure 16 and Table 10.

Table 10: Conditions for Test # 4

Experimental Data: Test # 4

<u>VARIABLE</u>	<u>TEST VALUE</u>
Slurry	5% SiO ₂ in demineralized water
Electrode Separation	14 inches
Chemicals	NaCl (according to test requirements)
Depth of Feed Well Discharge Port Below Cathode	1 inch
Temperature Range during test	18.7°C to 26.4°C
Ave. Volt Gradient	Change During Test
Ave. Power Input	Change During Test
Average Q _f	985 cc/min
Average Q _{of}	840 cc/min

Figure 16 includes both the relationships of voltage and power to overflow clarity. The voltage curve is particularly interesting as it illustrates the importance of mobility on zeta potential. At a high voltage gradient and low mobility the clarification in the overflow is quite poor but as the mobility increases, even with decreasing voltage gradient the clarity improves. Attempts to correlate imparted cataphoretic velocity with the

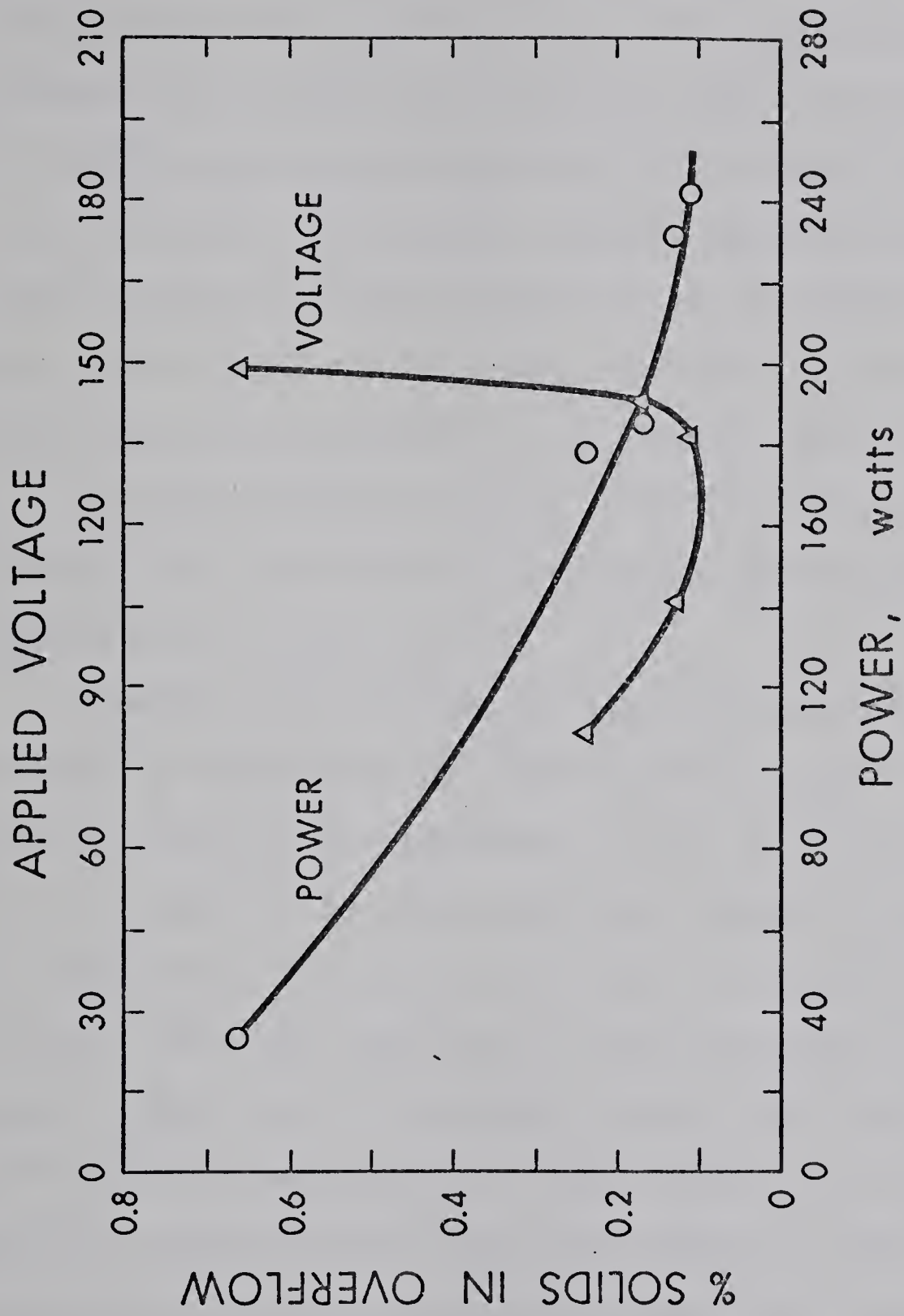


FIGURE 16: Overflow Clarity as a Function of Power and Voltage with Sodium Chloride Additions, for Test 4

clarity, by combining the data from Figures 15 and 16 would seem to indicate that clarity is a very complex function of the mobility. Good correlations could not be obtained for the equations upon which regression was done, probably due in some part with the error in interpolation to find the appropriate mobility from Figure 15. Nevertheless, a simple relationship between mobility and clarity under a given voltage gradient is not available probably due to the complex mechanisms involved in the cataphoretic deposition, as discussed in the results for Test no. 2.

In the region of constant mobility, (i.e. $[\text{Na}^+]$ 25 ppm) both the power and voltage curves resemble their counterparts in Test no. 2.

Another, and reoccurring inconsistency, here, is the failure to reproduce the results of Test no. 1. The same clarification as was achieved in Test no. 1 with tap water was not obtained in this test even though the mobilities are apparently larger in this case. This would seem to indicate that the mobility in the 5 per cent suspension used in Test no. 1 is somewhat larger than the $2.56 \times 10^{-4} \text{ cm}^2/\text{volt-sec}$ quoted in the illustrative calculation. This is probably true since this mobility value was obtained from Figure 5 which was done on a suspension of 2500 ppm silica while in the test suspension the solids concentration is 5 per cent. In effect this increase in solids concentration decreases the divalent cation concentration per unit weight of solid thus providing less

effective shielding and larger zeta potentials or mobilities.

The effect of NaCl concentration on Sf in this test is more complex than those previously discussed. With the exception of the case where there was no NaCl added to the system, resulting in a low ξ , the particle ξ was approximately constant. Thus, according to equation 5 changes in electro-osmotic velocity are proportional to changes in the electric field. Calculations show that Sf equals 6.9 per cent when the NaCl concentration is a minimum and that Sf equals 7.6 per cent in all the other cases. This means one of two things, either i) that the changes in the applied electric field are small resulting in a constant electro-osmotic velocity and hence a constant increased value of Sf, or ii) that electro-osmosis is only one mechanism whereby the raking efficiency and consequently the value of Sf is determined. In this case some other mechanism is predominant because changing electric fields produce no changes in Sf at constant ξ . Since the voltage gradient in those tests where Sf was observed to be constant, varies from a minimum of 2.04 volts/cm to a maximum of 3.76 volts/cm, alternative ii) must be selected. The exact mechanism responsible for the noted behaviour of Sf is a matter of speculation and will be considered as a characteristic of the experimental system.

In summary, the ionic strength of the suspension is very important since it plays an important role in determining the power input to achieve the required voltage gradient and it also determines the particle mobility. For systems similar to the silica one being tested, the concentration of divalent cations is extremely important in determining the clarification efficiency while for clay systems this consideration is less important.

Test # 5 - The Effect of Electrode Separation on Overflow Clarity

This test was designed to determine the effect of electrode separation on the overflow clarity. The procedure followed was to begin with the lowest separation possible and once steady state had been reached, the electrode was raised, using a ruler to insure parallelness of the electrodes. The results of this test are presented in Figure 17 and Table 11.

Table 11: Conditions for Test # 5

<u>VARIABLE</u>	<u>TEST VALUE</u>
Slurry	5% SiO ₂ in demineralized water
Electrode Separation	10"/12"/14"
Chemicals* Added	NaCl to 19.5 ppm Na ⁺ in slurry
Depth of First Feed Well Discharge Port Below Cathode	4"/6"/8"
Thick. Pulp Temp. Range	20 ⁰ C to 24.1 ⁰ C
Ave. Voltage Gradient	5.39/4.56/3.97
Ave. Power Input	237/216/199 watts
Ave. Feed Flowrate	1000 cc/min
Ave. Overflow Flowrate	840 cc/min

Figure 17 has two different ordinate scales which represent the same variable. The reason for this is that

* Determined by Atomic Absorbtion Spectroscopy

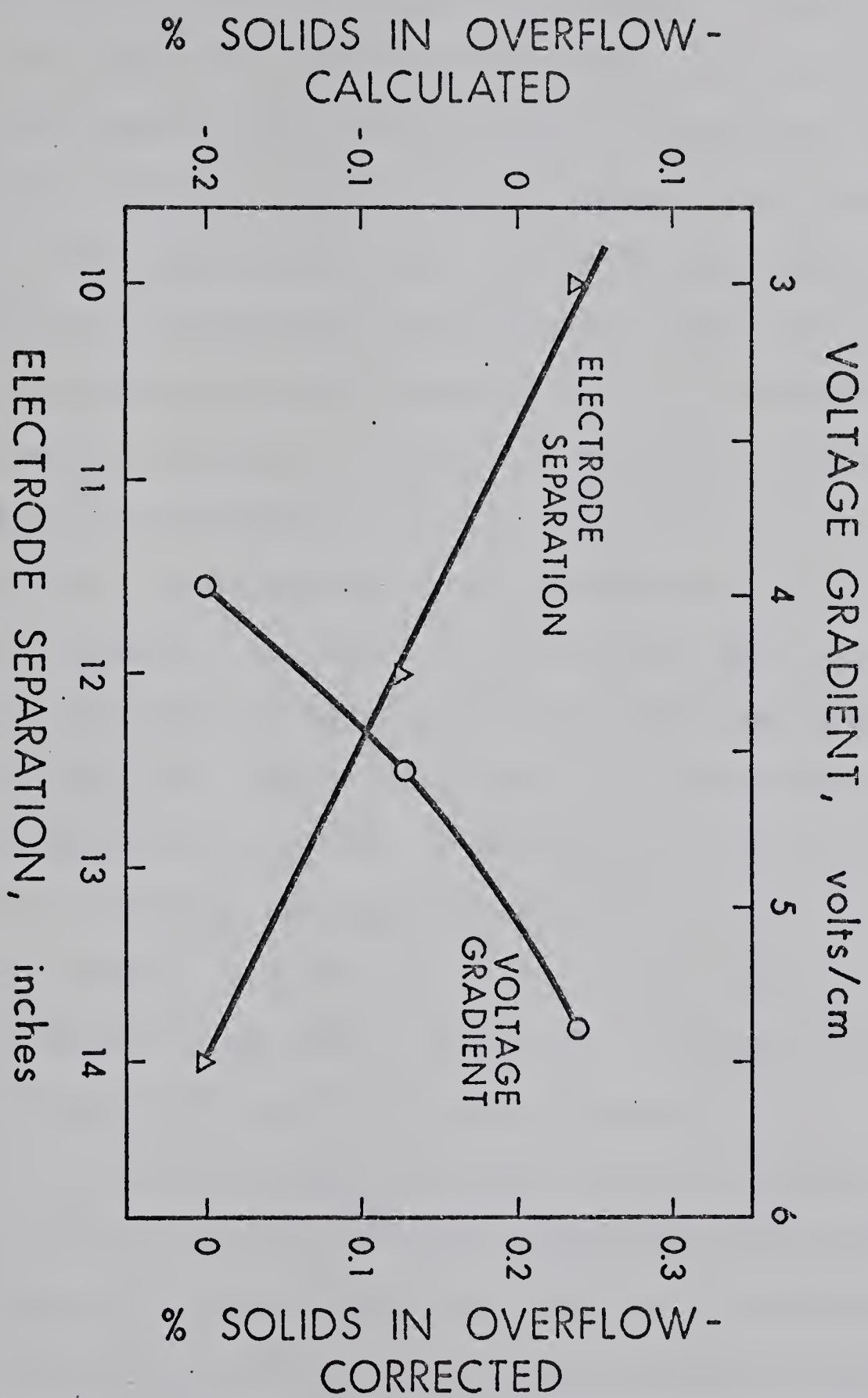


FIGURE 17: Overflow Clarity as a Function of Both Voltage Gradient and Electrode Separation, for Test 5

the left most scale shows negative values of S_o which is physically impossible. These negative results arose from employing equation [4] where the solution bulk density was less than that for water as determined from Figure 7. Since, experimental data for density vs. temperature for water is not available, the following method was used to 'correct' these negative values. The data from Figure 7 was subjected to regression under equation [9] with a resulting correlation coefficient of -1.00. Assuming the slope to remain constant, a new y intercept was calculated such that the most negative value of S_o could be set equal to zero. Using this equation, the density of water was recalculated for all the S_o calculations done and the results are those determined by the right most ordinate scale in Figure 17. The validity of this transformation is justified by the fact that, provided it is the soluble salts which result in this density difference and these salts are uniformly distributed in the water than it should follow the same curve, being only slightly displaced on the ordinate scale, as is shown in Figure 7.

This transformation has only the effect of adding 0.2 per cent to the values of the left most scale, as shown.

In Figure 17, the voltage gradient shows a nonlinear relationship with S_o and as the voltage gradient increases, S_o does as well. Since there is no change in particle mobility it would be expected that the reverse should be true (i.e. as voltage gradient increases; S_o should

decrease). It was shown in Figure 12 that most of the clarification is done in the low voltage ranges and therefore it might be suggested that, since all of the voltage gradients used in this test exceed that used in Test no. 2, the overflow clarity may be somewhat insensitive to voltage but it still would not exhibit the trend shown in Figure 17. The explanation for this observation is based on the separation between the cathode and the first feed well discharge port as a function of depth in the thickener. For example, with the minimum electrode separation the currents created in the thickener (see Fig. 4a) cause the suspension to be carried up through the cathode and consequently out of the applied voltage gradient, further, particles above the cathode are repelled upward to some extent. In any event, the particles do not have a relatively long retention time in the applied field and as a consequence the finer colloids can report to the overflow. Increasing the electrode separation, while holding the level of the first feed well discharge port constant, serves to include more of the currents within the electrodes and hence increase particle retention time in this area and increase the probability of deposition. Therefore it is desirable to have an optimum electrode separation with low level discharge in the thickener. The resistance of the upper levels in the thickener is constant and exceeds that of the lower level. (This is based on the 10 inches of slurry

below the cathode, in the first part of the test, and the 9 inches above it.) Therefore an increase in separation shows a decrease in power input with better clarification. There must, of course, be a limit to the separation where the voltage gradient falls below that which is required for good clarification.

In this test, very little change in S_f was observed and the change was probably due to experimental weighing errors. This follows when the electro-osmotic effect on S_f , indirectly through S_u , is considered, with the relatively small changes in power and voltage used in this test.

In summary, there is a critical or optimum electrode separation and level of feed discharge to the thickener, which will minimize power input but result in the desired overflow clarity.

Test # 6 - The Effect of Solids Concentration in the Feed on Overflow Clarity

This test was designed to give the relationship between overflow clarity and the solids concentration in the feed. The procedure followed was to run three separate tests at various solids concentrations. The results are presented in Figure 18 and Table 12.

Table 12: Conditions for Test # 6

<u>VARIABLE</u>	<u>TEST A</u>	<u>TEST B</u>	<u>TEST C</u>
Slurry	5% SiO ₂ in D.W.	10% SiO ₂ in D.W.	15% SiO ₂ in D.W.
Electrode Separation	14 inch	14 inch	14 inch
Chemicals Added	NaCl to 10 ppm	As for A	As for A
Depth of First Feed Well Discharge Port Below Cathode	8 inch	As for A	As for A
Thick Pulp Temp. Range	17.3 ⁰ C to 22.5 ⁰ C	22.1 ⁰ C to 25.1 ⁰ C	21.9 ⁰ C to 25.15 ⁰ C
Ave. Volt Gradient	4.19v/cm	4.16 v/cm	4.13 v/cm
Ave. Power Input	121 watts	135 watts	141 watts
Ave. Feed Flowrate	970 cc/min	1200 cc/min	1440 cc/min
Ave. Overflow Flowrate	835 cc/min	835 cc/min	850 cc/min

The results for the 5 per cent slurry with the power on gave negative values of S_o at steady state. The transformation described in Test no. 5 was used to correct

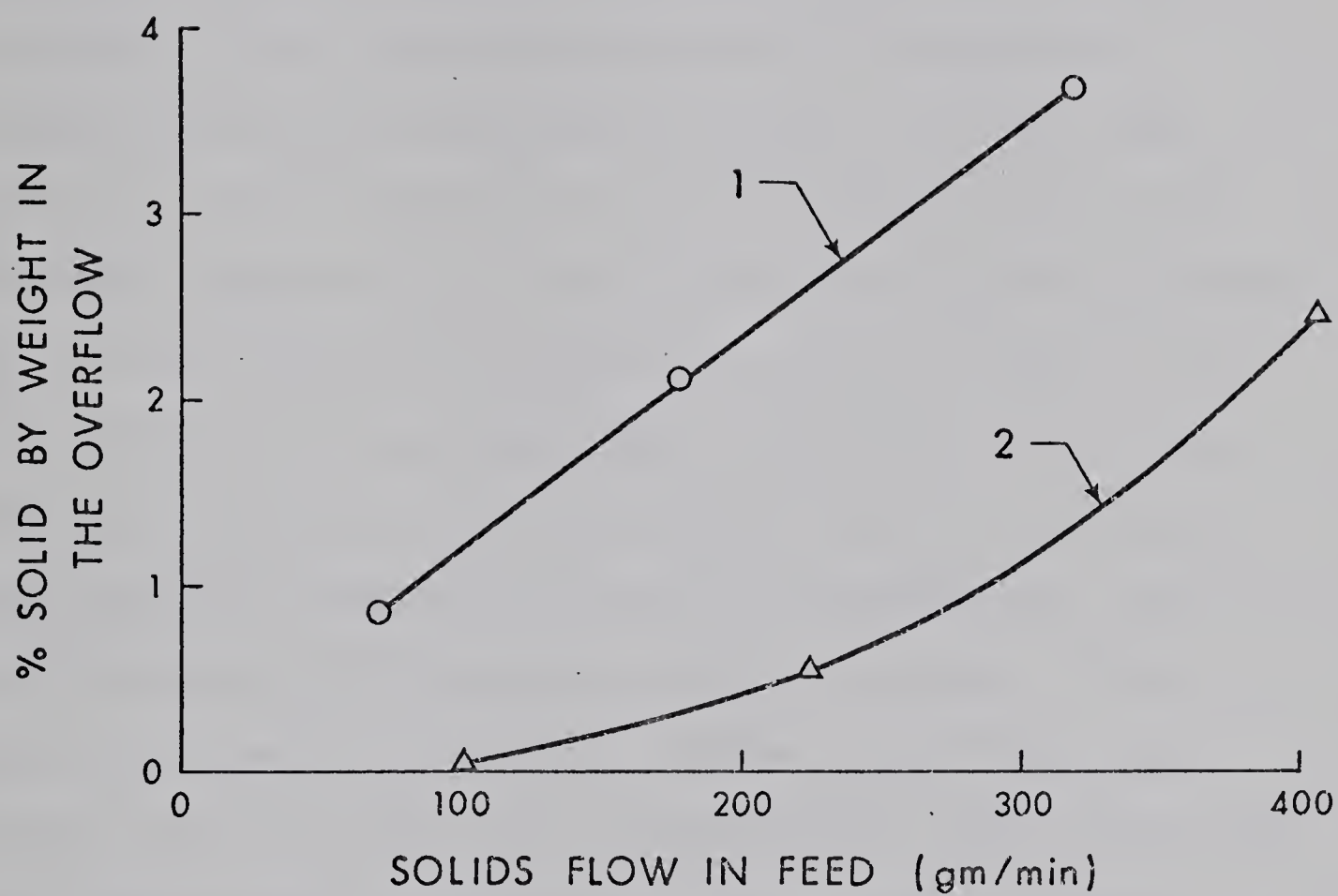


FIGURE 18: Overflow Clarity as a Function of Solids Feed-rate Both With and Without Cataphoretic Assistance; Test 6

all the results. Figure 18 shows the relationships between the corrected S_o values as a function of the mass flowrate of solids to the thickener, both with and without cataphoretic assistance.

The relationships of this curve are difficult to interpret quantitatively. There are two major reasons for this: i) at constant medium ionic strength, an increase in solids concentration causes, in this case, a reduction in the mobility since the weight ratio of the potential determining Cl^- ion to silica is greatly reduced, and ii) the increase in feed rate causes a change in the rate of circulation of the pulp within the thickener, the effect of which cannot be estimated since it is further complicated by changing the solids concentration. The clarification efficiencies for the 5 per cent, 10 per cent and 15 per cent nominal slurries are 99 per cent, 75 per cent and 33 per cent respectively. The curves show that increasing the solids feed rate to the thickener produces different effects depending on whether cataphoretic assistance is employed or not. Figure 18 shows that for the case where there is no cataphoretic assistance, S_o is linear with solids input to the thickener. (The minor variation in Q_o for Test C is assumed to have negligible effect on the final results.) The slope of curve 1 on figure 18 is very close to 1.0 which means that, under the conditions of these tests doubling solids input to the thickener will double S_o or nearly double S_o . This

latter remark may indicate that the thickener is more efficient at higher solids inputs, in the range studied, but the magnitude of the ratio change is small. In the second case, where cataphoretic assistance was employed the curve 2 on figure 18 shows an exponential increase in S_o with increasing solids input. This is due, in part, to the reduction in zeta potential caused by the reduction in the Cl^-/SiO_2 ratio as evidenced in Test no. 4. Using data from appendix 2 for Figure 18 it can be seen that when power was applied to a given slurry the value of S_f increased as would be expected:

In summary, the solids feed to such a system would be predetermined by the suspension to be treated. The clarification possible would be determined by; i) the size of the thickener and ii) the voltage gradient and iii) the particle mobility; the latter of which it may be possible to manipulate to a larger value without causing large power input increases.

C: Bentonite Tests

This test was designed to study the effectiveness of cataphoretic clarification on a slurry which contained a solid less amenable to this clarification process than the silica used in the previous tests. The solid chosen to use the slurry was bentonite because of its ability to form a stable colloidal suspension.

The preliminary test work completed before actual runs in the thickener apparatus were begun, consisted of establishing particle mobilities in both tap and demineralized water. The values obtained were $-1.48 \times 10^{-4} \text{ cm}^2/\text{volt} \cdot \text{sec}$ and $-2.6 \times 10^{-4} \text{ cm}^2/\text{volt} \cdot \text{sec}$ respectively. It was decided to run clarification tests with slurries made from both types of liquid.

The clarification tests gave some insight into the operability of the thickener apparatus. The first test, run under the conditions listed for Test no. 1, silica, using tap water to make up the slurry resulted in no detectable difference between the overflow and underflow with respect to solids content. Reduction of the Q_o/Q_f ratio showed no improvement in the overflow clarity and as a consequence it was decided that the particle mobility, achieved in tap water, was not large enough to allow a cataphoretic effect to take place within the thickener. The second test was designed to study the cataphoretic effect in demineralized water with a small Q_o/Q_f ratio.

The procedure was to run without power until steady state was reached and then turn on the power and determine the change in overflow clarity. The results of this test are presented in Figure 19 and Table 13 below.

Table 13: Conditions for Bentonite Test # 2

Experimental Data for Bentonite Test

<u>VARIABLE</u>	<u>TEST VALUE</u>
Slurry	2-1/2% Bentonite by wt. in demineralized water
Electrode Separation	14 in./35.6 cm
Chemicals Added	None
Depth of First Feed Well Discharge Port Below Cathode	8 inches
Thick. Pulp Temp. Range	20.7 ⁰ C to 22.95 ⁰ C
Ave. Volt Gradient	2.44 volts/cm
Ave. Power Input	195 watts
Ave. Feed Flowrate	780 cc/min
Ave. Overflow Flowrate	620 cc/min

Figure 19 illustrates the effect of cataphoretic assistance on clarification when the power is turned on. It is of importance to note at this point the extremely large Q_u/Q_o ratio. The design of the thickener apparatus has an inherent limit to the minimum feed rate below which a stable volumetric feed flow cannot be maintained. This required that in order to achieve an overflow rate which resulted in a net water flux upward, which could be overcome

by the imparted cataphoretic velocity, the underflow flowrate had to be abnormally large. To illustrate the difference in results for silica and bentonite the following calculation will be done. Figure 20 shows the split accomplished in the thickener apparatus. In the calculation the specific gravity of water has been assumed to be equal to one and, also, it is assumed that the underflow flowrate has negligible effects on the motion in zone 2 of the thickener. The last assumption allows calculation of the underflow flowrate which will yield 40 per cent solids in the underflow for bentonite for the purposes of this illustrative calculation. (The data used in the calculations was taken from Table 4 and Table 13; the underflow was set at 40 per cent solids and the flowrates Q_u and Q_f calculated.)

The clarification achieved with the bentonite, shown on Figure 19, is $(1.65 - 0.96)/1.65 * 100$ per cent = 41.8 per cent while with silica the clarification was 96 per cent. Further, the silica was slurried in tap water at 5 per cent solids while the bentonite was mixed in demineralized water at 2-1/2 per cent solids.* The unit area ratio shows that to achieve 41.8 per cent clarification of bentonite under the conditions of the test requires a thickener with 9.5

*The bentonite was slurried at a lower solids content than the silica to reduce viscous effects resulting from swelling and also to ease handling.

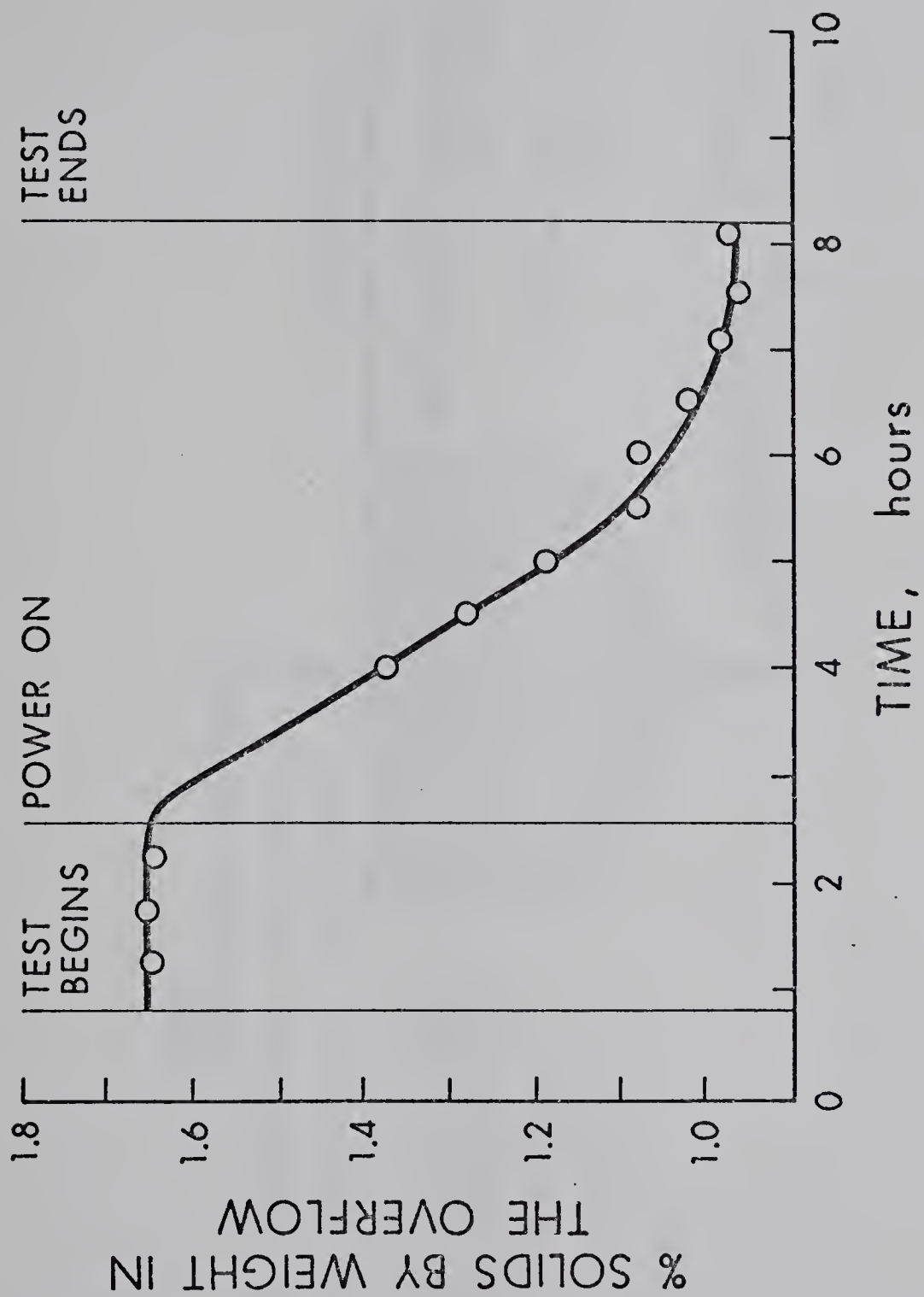


FIGURE 19: Overflow Clarity Versus Time for the Bentonite Test 2

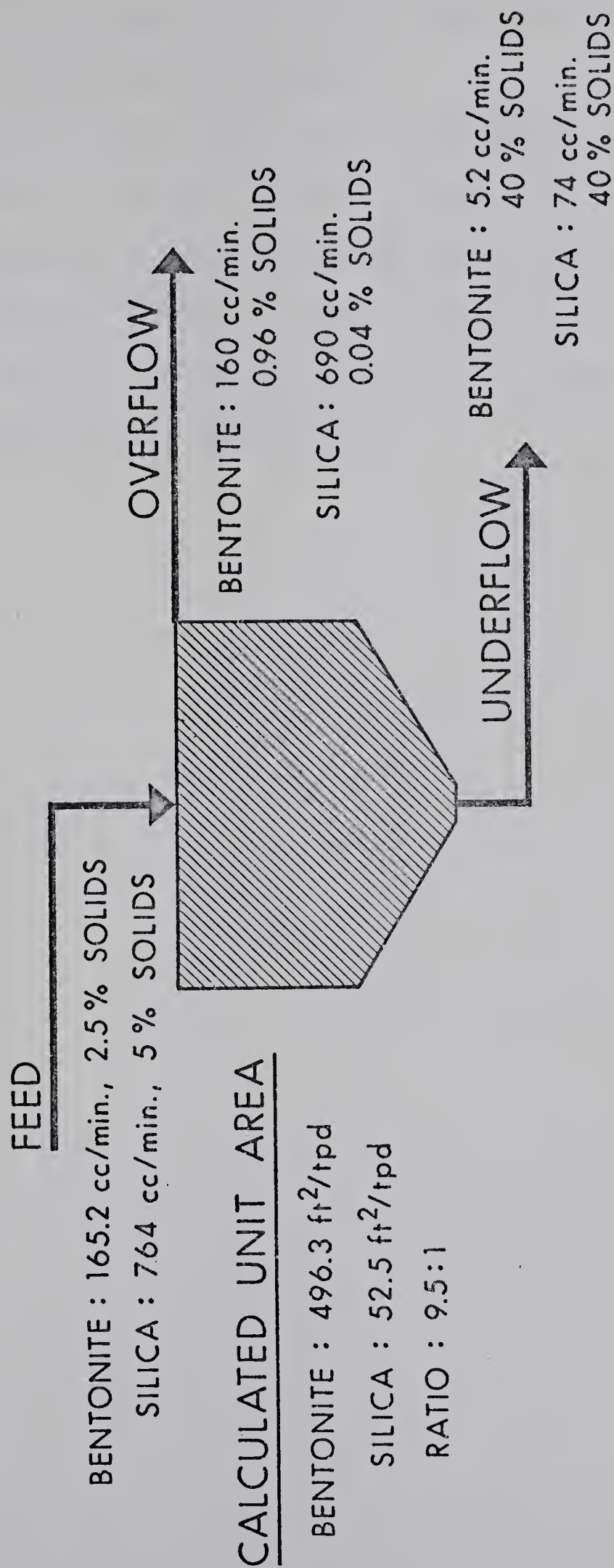


FIGURE 20: An Illustration of the Effectiveness of the Experimental Apparatus in Treating Bentonite and Silica Suspensions

times the area of one which could treat the same silica tonnage with much better results.

It has been shown that such a system as was used for experimentation in this project, is able to treat a bentonite suspension to some degree, but, to obtain good clarification (~90 per cent), the capital and power would most probably be so uneconomic as to make such an industrial application impractical.

D: Great Canadian Oil Sands Test

This, the final test, was conducted with a sample of the tailing product obtained from the Great Canadian Oil Sands (G.C.O.S.) plant in Fort MacMurray in north-eastern Alberta, during July of 1973. A brief introduction is necessary before giving the experimental results.

The stimulus for approaching the project discussed in this work was provided by the problems presently being encountered by the G.C.O.S. plant. G.C.O.S. was the first plant to begin producing synthetic crude oil from the bitumen sands of the area. These 'tar sands' consist of sand, heavy crude oil and clay minerals. After substantial removal of the crude oil the sand and clay slurry is pumped to a tailing pond where the coarse sand particles settle and the fine clay remains in suspension. The presence of the clay fraction in the water precludes recycling as this leads to processing problems the most notable of which are:

i) Fouling of the heat exchangers; the preliminary step in extraction requires a water temperature of approximately 180°C . The fouling lowers the overall heat transfer coefficient between the chambers and requires frequent cleaning of the exchangers and thus large production losses; and,

ii) A buildup of clay in the recycle water serves to increase the viscosity of the suspension. To enable good

operation of the flotation cells in the plant the middling viscosity must be limited to about four centipoise.* The viscosity changes very rapidly beyond the clay loading limit of the water which results in the sudden change from an operable to an inoperable condition.

The net result of these problems is that the consumption of river water increases and the area of tailings impoundment exceeds design expectations. It has recently been stated that the present Alberta government expects three plants to be producing synthetic crude on the 'tar sands' by 1982 and that by the year 2000 there will be twenty plants in production. Many of these plants will be larger than the present G.C.O.S. plant and thus there is a strong possibility that the clay suspension problem will greatly manifest itself assuming no major technological advance in the extraction flowsheet is forthcoming.

The research staff at G.C.O.S. have investigated many different clarification techniques to reduce the solids concentration of the tailings pond water, but, as yet, those which have been seen to work are economically prohibitive. Some of the techniques which have been studied include flocculation, x-ray bombardment, centrifuging, freezing out, and an application of the cataphoretic technique. It was obvious that a cheap reliable method was

*A more complete discussion of the flotation problem can be found in Clay Mineral Concentration in Tailings of G.C.O.S., B.W. Raymond M.Sc. thesis Montana Coll. of Min. Sci. & Tech. May 1969.

needed for solution to this problem and this initiated the investigation of cataphoretic assistance in the clarification of a colloidal suspension, in a thickener.

The results of the test work conducted with the G.C.I.S. sample are shown in Figure 21 and Table 14.

Table 14: G.C.O.S. Test Data

<u>VARIABLE</u>	<u>TEST VALUE</u>
Slurry	G.C.O.S. sample at 2.4% solids*
Electrode Separation	14 in./35.6 cm.
Chemicals Added	None
Depth of First Feed Well Port Below Cathode	8 inches
Temperature Range	19.8 ⁰ C to 26.4 ⁰ C
Ave. Volt. Gradient	7.43 volts/in - 2.93 volts/cm
Ave. Power Input	250 watts
Ave. Feed Flowrate	735 cc/min
Ave. Overflow Flowrate	165 cc/min

Figure 21 illustrates that a 52.5 per cent clarifying efficiency is achieved under the test conditions. Since power costs were desirable for this test relative resistance measurements were taken on centrifuged aliquots of both the thickener overflow and the G.C.O.S. sample. These values

*The physical nature of the sample required it be transported in slurry form to the mixing reservoir. The sample solids density was taken as 2.45 and the solids content of the slurry measured, using this value, allowing the appropriate dilution for testing.

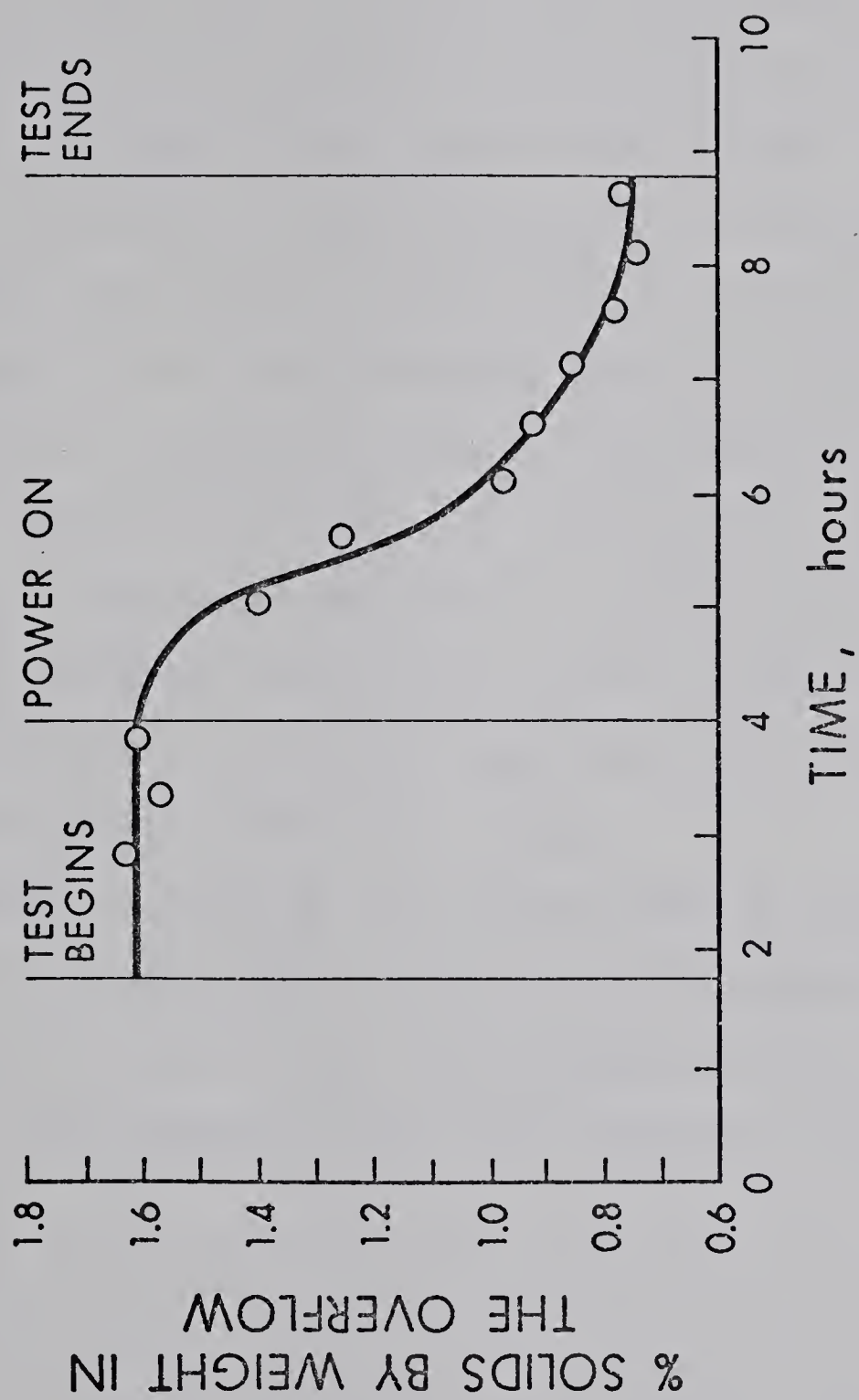


FIGURE 21: Overflow Clarity Versus Time for the Great Canadian Oil Sands Test

were 3,000 ohms and 1,650 ohms respectively (i.e. the G.C.O.S. sample is 1.82 times more conductive than the test liquid and this will require 1.82 times the power to maintain the same voltage gradient based on equation (6). Calculations show that to treat 1000 U.S. gallons on the test apparatus the cost would be 0.85 dollars, assuming a power cost of 0.005 dollars per kilowatt hour. This is a high unit cost for a relatively poor clarification. This, coupled with the initial capital cost to fabricate an industrial model of the clarification apparatus would appear to make this an economically undesirable means of combating the clay suspension problem. It is of interest to note that the ion content of the water is particularly important for power considerations but the cation concentration does not show an effect on particle mobility near the magnitude of that exhibited in the silica tests.

In summary, although this method does not appear to be industrially applicable to the G.C.O.S. problem in its present form, it may be the least expensive means of clarifying when compared with those methods previously mentioned.

CONCLUSIONS

The apparatus designed to clarify colloidal suspensions using cataphoresis to assist gravitational sedimentation was demonstrated to work in principle.

The conclusions which can be drawn with respect to the operation of a system of this nature, as were determined in the silica tests, are:

- i) There is an optimum voltage gradient (or power input), which is determined by the characteristics of the suspension. For a given suspension the overflow clarity will increase in an exponential manner as either voltage or power is increased.
- ii) The rate of treatment of a suspension should be held to the lowest practical value to minimize overflow flowrate and hence maximize clarity.
- iii) The ionic strength of the suspension should be controlled, where possible to optimize the combination of minimizing power input and maximizing particle mobility.
- iv) The separation between the upper electrode and the feed well discharge level should be large enough to prevent particles from reporting to the overflow by short circuiting due to internal currents while keeping a sufficiently large voltage gradient.
- v) The solids flux or feedrate must be held to the

lowest practical value.

The electro-osmotic effect which assists in the dewatering of the underflow deposit is beneficial with respect to thickening the suspension. This effect was detrimental to the results in this test since the equipment was operating in a continuous closed circuit such that increases in S_u caused subsequent increases in S_f and to some extent masked the effect of cataphoretic assistance.

The apparatus was also shown to work in the clarification of two clay suspensions, although, because of the power restrictions in this testing, good clarification could not be achieved.

To compare the clarifying efficiency, operating costs for systems to treat the three suspensions used in this testwork, Table no. 15 is presented.

This table is subject to the following conditions; i) The results of tests no. 1, C and D and ii) A power cost of 0.005 dollars per kw-hr iii) A solids flow to the clarification process of 3100 t.p.d* iv) 40 per cent solids by weight in the underflow v) The cost is taken from (36) with 50 per cent added on for electrodes, suitable tank lining and instrumentation.

The table shows the silica to have the best economics and efficiency while the other two suspensions are relat-

*Typical of the flow of solids in the recycle water at G.C.O.S.

TABLE 15: Comparative Economics and Efficiencies for Suspensions Treated

Suspension	Nominal Solids Conc by wt.	Cost to Treat 1000 U.S. Gal at given Efficiency	Calculated Thickener-Clarifier Unit Area	No. of Thickeners Required and Diameter	Est. Capital Cost of These Units
Silica in Edmontonton City Tap Water	5.0%	\$0.103 96%	52.5 ft ² /tpd	4 225 ft	\$ 1,554,000
Bentonite in Demineralized Water	2.5%	\$0.372 41.8%	496.3 ft ² /tpd	38.7 225 ft	\$15,034,495
G.C.O.S. Clay in Mother Liquor	2.4%	\$0.850 52.5%	493 ft ² /tpd	38.5 225 ft	\$14,957,250

ively similiar. Based on these comparative studies it would have to be concluded that the prohibitive economics and poor application achieved with the clay suspensions would preclude any industrial application of a cataphoretically assisted thickener for clarification at the present time.

With regard to the G.C.O.S. suspension, this method works to some extent to both clarify liquid through catophoresis and compact sludge through electro-osmois. These are the desired aims of a process to treat sludge, but in this case the solids content of the feed was well below that which would have to be treated in practice (S_f equals 5 to 30 per cent). The increase in S_f could have a deleterious effect on system performance and hence make industrial application an even less likely prospect.

The apparatus has been demonstrated to work in the clarification of colloidal suspensions, although, with the present design, the results obtained rule out practical applications based on performance and economic considerations.

REFERENCES

1. SPEIL, S., THOMPSON, M.R. Electrophoretic Dewatering of Clay. Ceramic Age Oct: pp 106, 1942.
2. SPEIL, S. Discussion on Electrophoretic Dewatering of Clay Suspensions. Bull. Am. Ceram. Soc. 20: No. 7, pg. 244-45, 1941.
3. SPEIL, S., THOMPSON, M.R. Electrophoretic Dewatering of Clay. Trans. Electrochem. Soc. 80: pg. 119-45, 1941.
4. RALSTON, O.C., HOSEH, M. Electrophoretic Filtration of a Kaolin Slurry. Trans. Electrochem. Soc. 80: pg. 85-93, 1941.
5. HOUSTON, E.C., JONES, V.J., POWELL, R.L. Electrical Dewatering of a Phosphate Tailing. Trans. A.I.M.E. Mining Transaction. 184: pg. 365-70, 1949.
6. MACKENZIE, J.M.W. Zeta Potential Studies in Mineral Processing: Measurement, Techniques, and Applications. Minerals Sci. Engng. 3: No. 3, pg. 25-43, July 1971.
7. PARKS, G.A., DEBRUYN, P.L. Zero Point of Charge of Oxides. J. Phys. Chem. Ithaca. 66: pg 967-73, 1962.
8. VAN OLPHEN, H. In: An Introduction to Clay Colloid Chemistry. Interscience: New York, 1963. pg. 80.
9. PARKS, G.A. Aqueous Surface Chemistry of Oxides and Complex Oxide Minerals. In: Equilibrium Concepts in Natural Water Systems. Washington, Am. Chem. Soc. 1967, Advances in Chemistry Series, No. 76, pg. 121-60.
10. QUIRK, J.P. Negative and Positive Adsorption of Chloride by Kaolinite. Nature 188: pg 253-54, 1960.
11. COUGHANOUR, W.L., UTTER, J.L. Cataphoresis of Purified, Fractionated Kaolinite Particles. J. Am. Ceram. Soc. 27: No. 4, pg. 116-20, 1944.
12. HAUSEN, E.A., LEBEAU, D.S. Studies in Colloidal Clays II. J. Phys. Chem. 45: No. 1, pg. 54-64, 1941

13. MOORE, W.J. In: Physical Chemistry, 3rd Edition, Prentice Hall, Englewood Cliffs, N.J. (1962) pg. 751.
14. KORTU,, G., BOCKRIS, J.O.M. In: Textbook of Electrochemistry Vol. II, Elsevier Pub. Co., Houston (1951) pg. 353.
15. BOCKRIS, J.O.M., DEVANATHAN, M.A.V., MULLER, K. On the Structure of Charged Interfaces. Proc. Roy. Soc. Lond. 274: pg. 55-79, 1963
16. FRUMKIN, A.N., et al. Dokl. Akad. Nauk. SSSR. 115: pg. 751, 1957.
17. KIM, M.K. Flotation Behaviour of Barite With Adsorbed Fatty Acids. M.Sc. Thesis, The University of Alberta, Edmonton, Alberta, Canada. (1972) pg. 91-94.
18. RIDDICK, T.M. In: Control of Colloid Stability through Zeta Potential. Livingston Pub. Co., Wynnewood, Penn. (1968) Chaps. 8 and 9.
19. SMITH, R.W., TRIVEDI, N. Variation of Point of Zero Charge of Oxide Minerals as a Function of Aging Time in Water. Soc. Min. Engrs. A.I.M.E. Preprint: 72-B-26.
20. DANIELL, J.F., PANKHURST, K.G.A., RIDIFORD, A.C. IN: Recent Progress in Surface Science Vol. I. Academic Press, New York (1964) pg. 94.
21. HANED, H.S., OWEN, B.B. In: The Physical Chemistry of Electrolyte Solutions. Reinhold Pub. Corp. New York (1963).
22. SHAW, D.J. In: Introduction to Colloid and Surface Chemistry. BuHerworths, London (1966), Chap. 7.
23. JIRGENSONS, B., STRAVMANIS, M.E. In: A Short Textbook of Colloid Chemistry. Macmillan Co., New York. (1962) Chap. 7.
24. ADAMSON, A.W. In: Physical Chemistry of Surfaces. Interscience Pub. Inc., New York (1960), Chap. IV.
25. KRUYT, M.R. Irreversible Systems In: Colloid Science Vol. I. Elsevier, New York (1952), pg. 198.

26. OVERBECK, J. TH. In: Advances in Colloid Science
Vol. III. Interscience Publishers Inc. New York,
(1959).
27. COE, H.S., CLEVENGER, G.H. Method for Determining
the Capacities of Slime Settling Tanks. A.I.M.E.
Trans. 55: pg. 356, 1916.
28. TALMADGE, W.P., FITCH, E.B. Determining Thickener
Unit Areas Ind. & Eng. Chem. 47: pg. 38, 1955
29. FITCH, B.W. Unsolved Problems in Thickener Design
and Theory A.I.M.E. Preprint 71-B-111.
30. SCOTT, K.J. Mathemstical Models of Mechanism of
Thickening Ind. & Eng. Chem. Fund. 5: No. 1,
pg. 109, 1966.
31. CROSS, H.E. A New Approach to the Design and
Operation of Thickeners. J.S. Afr. Inst. Mm.
Metall. 63: pg. 271-98, 1963.
32. ANDERSON, A.A., SPARKMAN, J.E. Review Sedimentation
Theory In: Chemical Engineering, Nov. 2, 1959.
33. BERRY, L.G., MASON, B. In: Mineralogy; Concepts,
Descriptions and Determinations. W.H. Freeman
& Co., San Francisco, (1959) pg. 508-9.
34. EITEL, W. In: The Physical Chemistry of the
Silicates. Univ. Chicago Press, Chicago (1954),
Section AIII, pg. 69.
35. SIENKO, M.J., PLANE, R.A. In: Chemistry: Principles
and Properties McGraw-Hill Book Co., Toronto (1966)
pg. 478.
36. PARKINSON, E., MULAR, A. In: Mineral Processing
Costs and Preliminary Capital Cost Estimations
Vol. 13 Canadian Institute of Mining and
Metallurgy., (1972) pg. 102.

APPENDIX 1

ILLUSTRATION OF THE CONTINUOUS
CATAPHORETICALLY ASSISTED
THICKENER SYSTEM

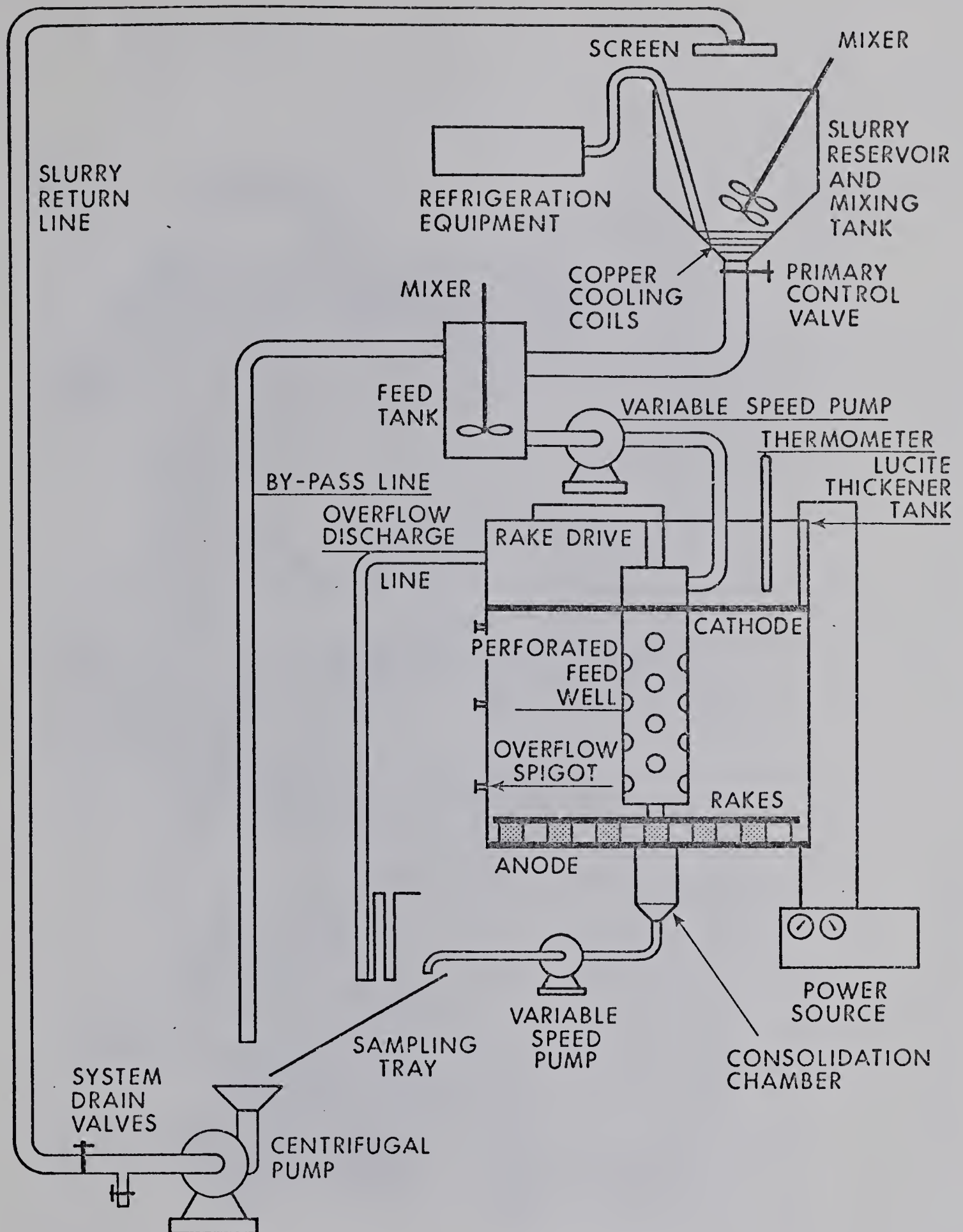


Figure 22: Schematic of the Cataphoretically Assisted Thickener Clarifier Apparatus

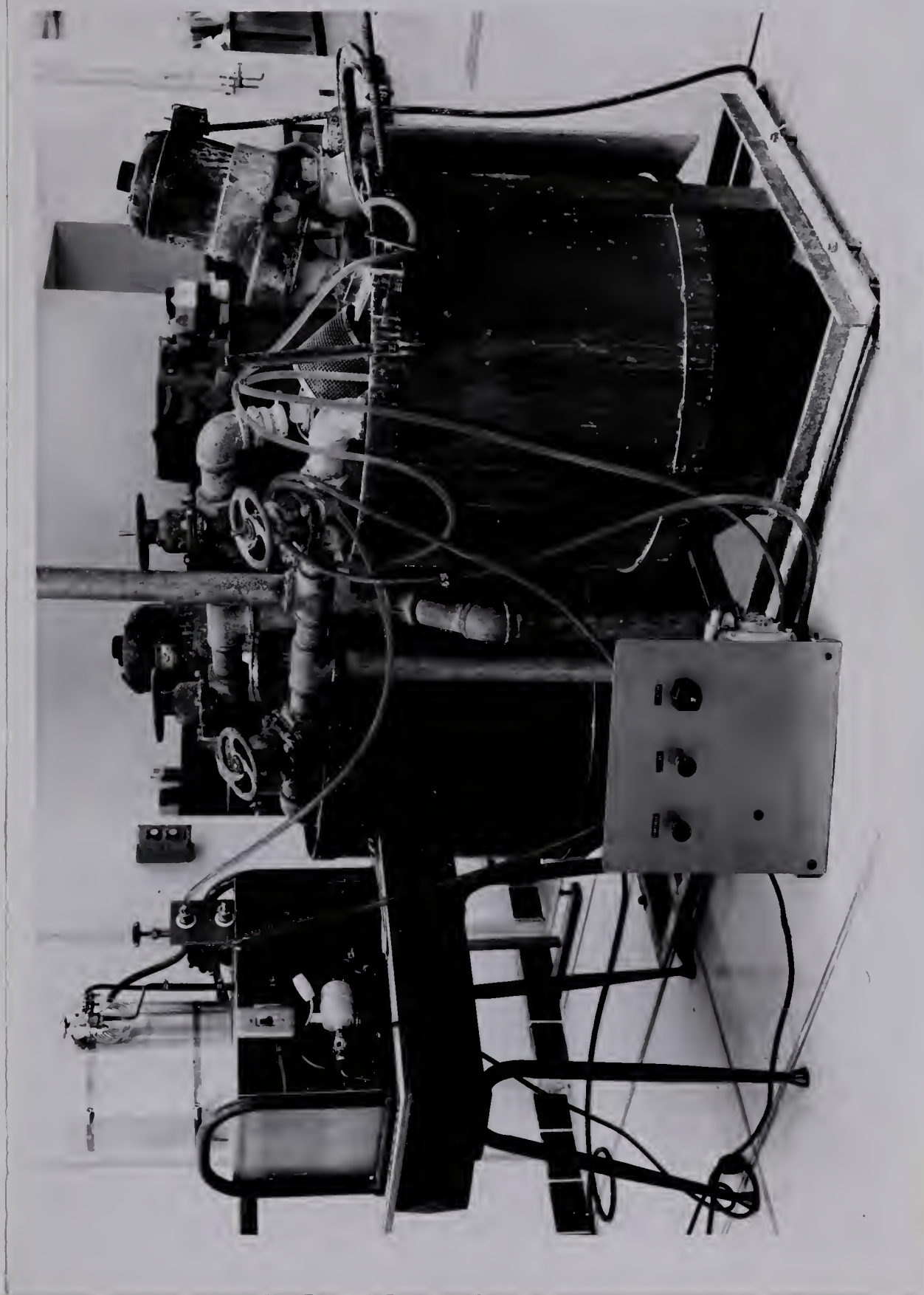


PLATE 1: The Slurry Reservoir Tank and Refrigeration Equipment

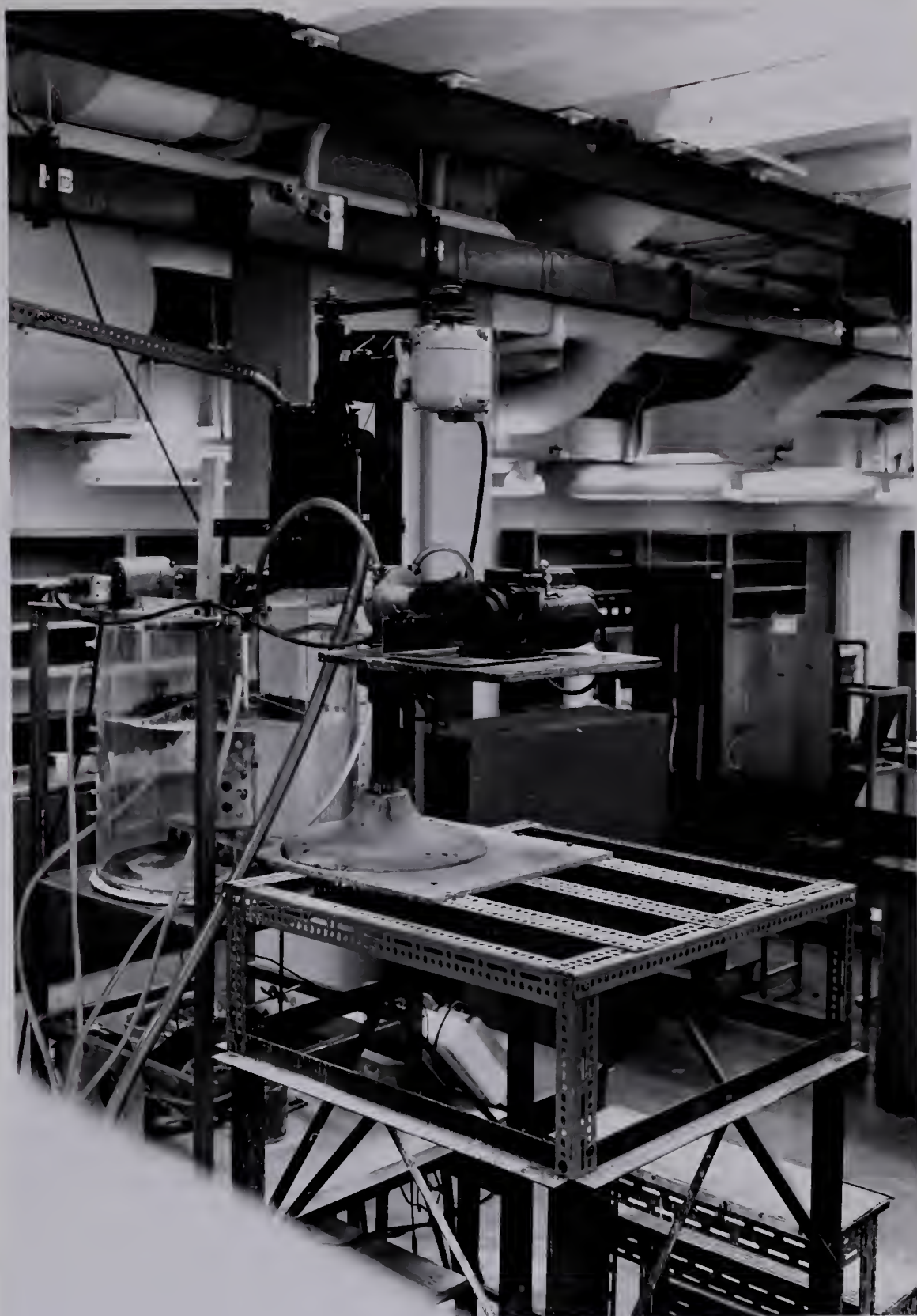


PLATE 2: The Slurry Feed System

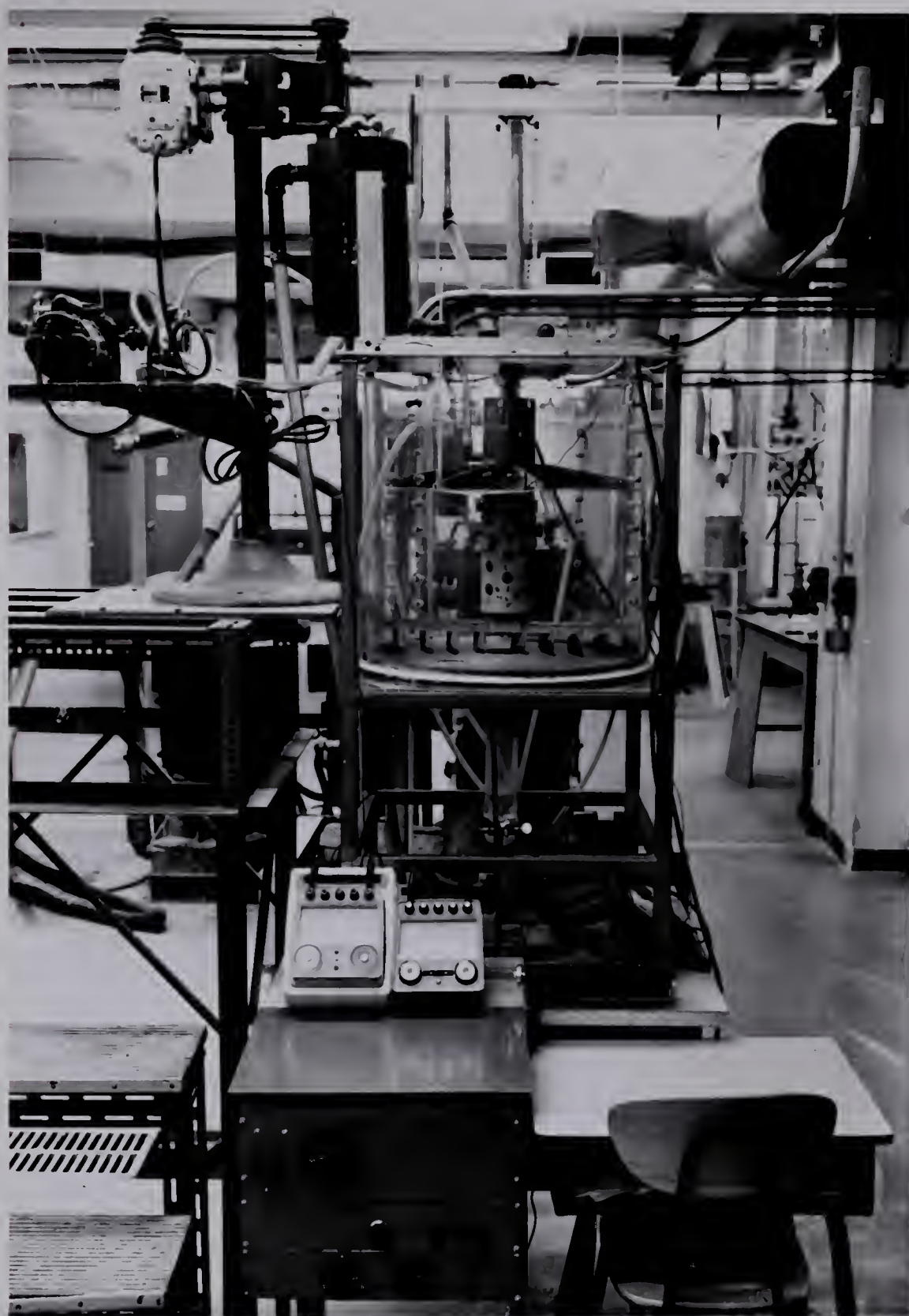


PLATE 3: The Thickener and Power Source

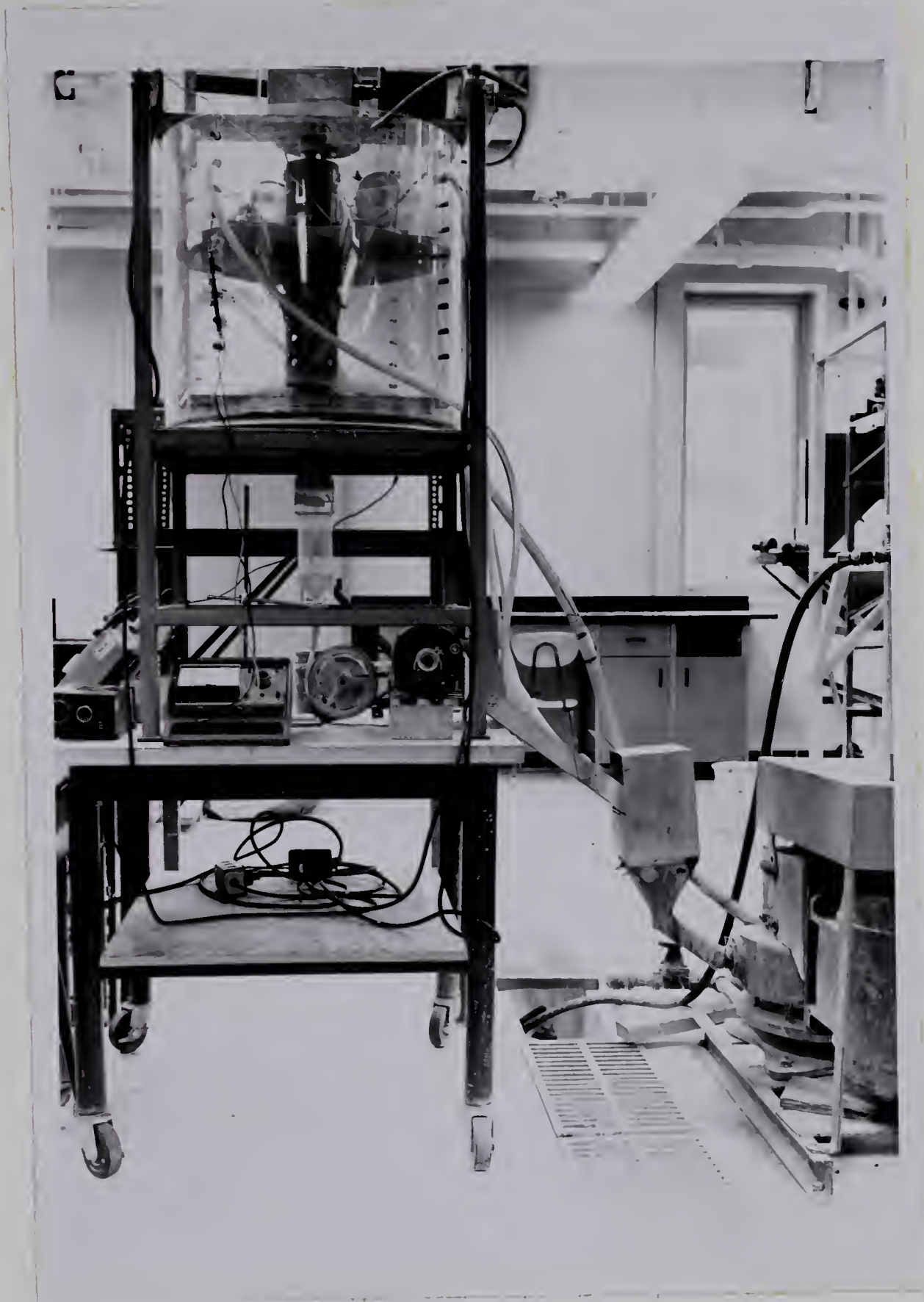


PLATE 4: The Underflow and Slurry Return Pumps

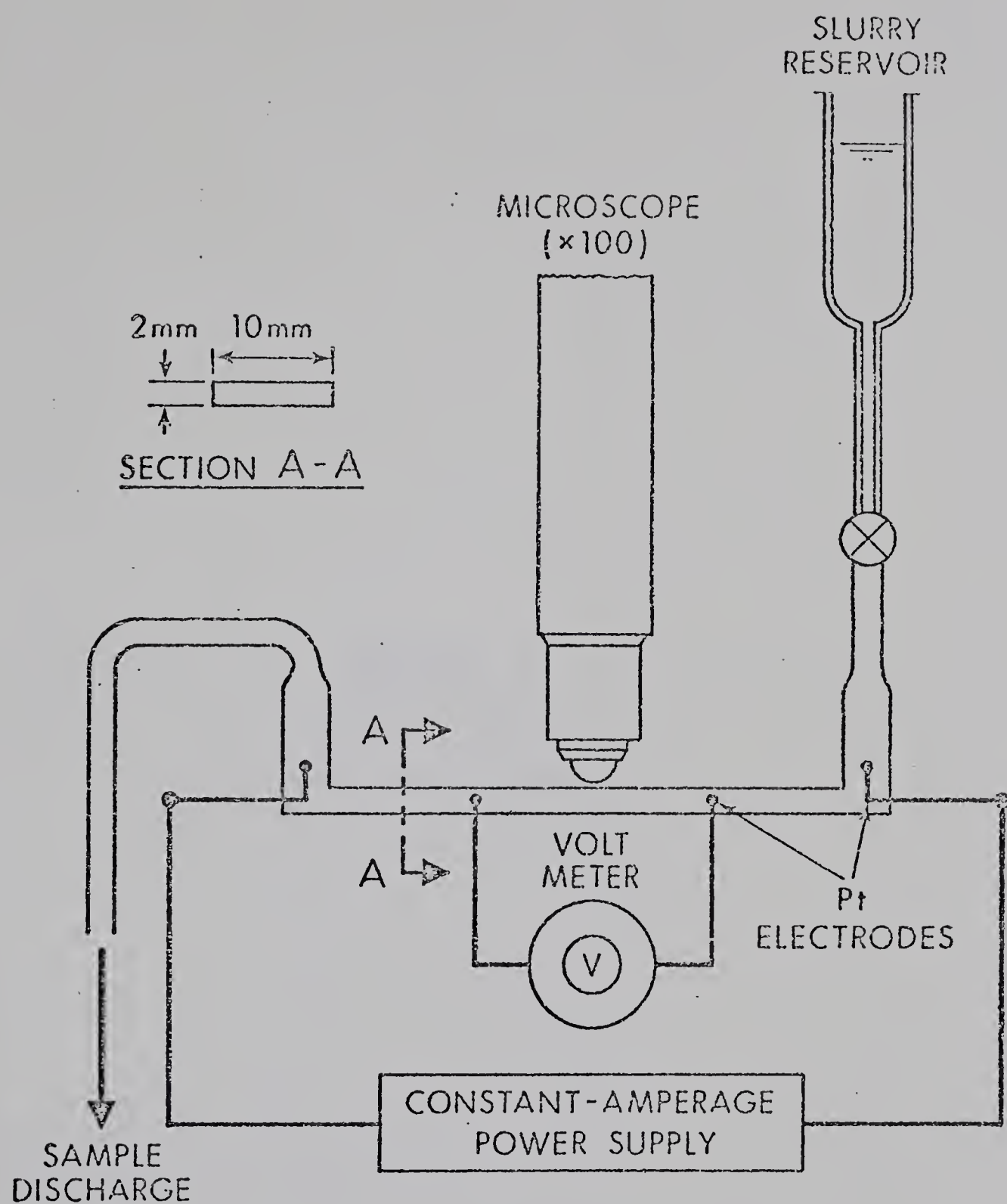


FIGURE 23: Schematic Illustration of Mobility Measurement Apparatus

APPENDIX 2

DATA FOR FIGURES

Figure #5

<u>cm² Mobility</u> <u>volt-sec x 10⁻⁴</u>	<u>pH Value</u>	
-1.98	3.11	
-2.45	3.91	
-2.66	5.06	
-2.55	6.0	Comments: 2500 ppm suspension of -400 Mesh SiO ₂ in Edmonton tap water.
-2.62	7.0	
-2.58	8.05	
-2.53	9.1	
-2.25	10.01	
Natural	11.02	
Flocculation	11.98	

Figure #6A. Cyclosizer Data

<u>Cummulative</u> <u>% Passing</u>	<u>Passing Size</u> <u>in Microns</u>
99.9	49
97.8	35.2
87.2	27.2
65.0	17.8
52.8	13.5

B. Hydrometer Data

<u>Cummulative</u> <u>% Passing</u>	<u>Passing Size</u> <u>in Microns</u>
99.9	59.6
95.9	42.7
86.9	31.1
74.3	22.8
61.7	17.9
56.5	14.5
49.2	12.2
41.0	9.9
32.9	7.2
27.6	5.4
24.8	4.7
21.5	3.9
11.0	1.6

Comments: Cyclosizer used with
the compliments of Brenda Mines
Ltd., Peachland, B.C. Canada.

Figure #7

<u>Temperature $^{\circ}\text{C}$</u>	<u>Density of Water</u>
18 $^{\circ}\text{C}$	0.99862 gm/cc
19	0.99843 gm/cc
20	0.99823 gm/cc
21	0.99802 gm/cc
22	0.99780 gm/cc
23	0.99757 gm/cc
24	0.99733 gm/cc
25	0.99708 gm/cc
26	0.99682 gm/cc
27	0.99655 gm/cc
28	0.99627 gm/cc
29	0.99598 gm/cc
30	0.99568 gm/cc
31	0.99537 gm/cc
32	0.99506 gm/cc
33	0.99473 gm/cc
34	0.99440 gm/cc
35	0.99406 gm/cc
36	0.99371 gm/cc

Figure #8

<u>Time (hrs) Feed</u>	<u>Slurry Temp. ($^{\circ}\text{C}$)</u>	<u>Thick. Pulp Temp. ($^{\circ}\text{C}$)</u>
0.1	21.4	21.1
0.4	21.55	21.2
0.6	21.65	21.2
1.04	21.80	21.3
1.26	21.9	21.4
1.54	21.82	21.45
1.86	21.82	21.55
2.02	21.82	21.6
2.24	21.82	21.7

Figure #8 (cont'd)

<u>Time (hrs) Feed</u>	<u>Slurry Temp. (°C)</u>	<u>Thick. Pulp Temp. (°C)</u>
2.64	21.85	21.8
2.99	21.90	21.8
3.25	21.90	21.9
3.59	21.90	21.95
3.76	21.90	21.95
4.11	21.90	21.95
4.66	21.95	21.95
4.93	21.95	21.95
5.25	21.97	21.95
5.64	22.00	21.95
5.97	22.02	22.05
6.24	22.02	22.3
6.40	22.02	22.46
6.78	22.05	22.87
7.08	22.10	23.25
7.59	22.25	23.95
7.92	22.35	24.30
8.42	22.50	24.60
8.84	22.52	25.00
9.31	22.61	25.35
9.65	22.80	25.50
9.99	22.95	25.70
12.89	22.75	23.80

Comments: Test begins at 3.33 hrs, power on at 6.0 hrs,
power off at 10.0 hrs.

Figure #9

<u>Time (hrs)</u>	<u>Su</u>	<u>Underflow Pump Speed</u>
3.38	43.8	3.64 r.p.m.
3.82	44.8	3.64 "
4.14	44.5	3.64 "
4.68	44.8	3.64 "
5.28	43.1	3.64 "
5.70	44.7	3.64 "
6.42	42.2	3.64 "
7.70	49.6	3.64 "
8.00	53.0	3.64 "
8.08	-	8.7 "
8.52	37.1	8.7 "
8.59	-	7.32 "
9.04	42.4	7.32 "
9.57	42.4	7.32 "
9.89	45.7	7.32 "
9.94	-	8.7 "
12.91	33.6	

Figure #10

<u>So</u>	<u>Time (hrs)</u>
0.90	3.89
0.87	4.76
0.88	5.11
0.93	5.50
0.93	5.76
0.04	7.97
0.06	8.89
0.00	9.43
0.03	9.78
0.52	12.92

Figure #11

<u>So</u>	<u>Time (hrs)</u>	<u>So</u>	<u>Time (hrs)</u>
0.91	3.0	0.01	12.13
1.04	3.43	0.01	12.61
0.90	4.02	0.02	14.02
0.92	4.40	*0.02(Su = 44.8%)	14.22
0.90	5.36	0.09	15.11
0.93	5.83	0.12	15.56
0.91	6.11	0.07	16.20
*0.92(Su = 38.2%)	6.40	*0.09(Su = 42.1%)	16.40
0.12	7.28	0.20	17.22
0.04	7.83	0.23	17.67
0.01	8.43	0.18	18.00
0.01	8.89	*0.20(Su = 40.1%)	18.15
0.01	9.35	0.23	19.00
0.01	9.83	0.50	19.83
*0.01(Su = 50.2%)	10.0	0.72	21.08
0.05	11.55		

*Average values when power changes are made, as discussed earlier.

Figure #12

<u>So</u>	<u>Applied Voltage</u>
0.92	0
0.01	118
0.02	82
0.09	60
0.20	41

Figure #13

<u>So</u>	<u>Power in Watts</u>
0.92	0
0.01	266
0.02	127
0.09	60
0.20	28

Figure #14

<u>So</u>	<u>Qo cc/min</u>	<u>Su</u>	
0.51	820	39.8	Comment: Qo = 820 cc/min with no power; So = 0.90. Su = 36.5% with no power Qu = 150 cc/min in all tests
0.72	980	43.3	
0.80	1110	46.7	
0.90	1270	50.2	

Figure #15

<u>Mobility</u> <u>(cm²/volt-sec) x 10⁻⁴</u>	<u>Na⁺ Conc.</u> <u>in p.p.m.</u>	
-2.5	0	Comment: Samples of 5% SiO ₂ prepared by technique described in (18) pg. 30 with the exception that centrifuging replaced filtration.
-2.76	3.4	
-3.13	6.5	
-3.47	11.9	
-3.75	23.8	
-3.83	65.0	

Figure #16

<u>So</u>	<u>Applied</u> <u>Voltage</u>	<u>Power</u> <u>(watts)</u>
0.60	149	33
0.17	143	186
0.11	136	243
0.13	106	232
0.24	82	178

Figure #17

<u>Measured So</u>	<u>*Corrected So</u>	<u>Voltage Gradient volts/cm</u>	<u>Electrode Separation inches</u>
0.04	0.24	5.39	10
-0.07	0.13	4.56	12
-0.20	0.0	3.97	14

*Equation to correct water density is:

$$(H_2O) = -0.000236 T^{\circ}C + 1.001763$$

Figure #18

<u>Solids Flowrate to Thickener (gm/min)</u>	<u>So Without Assistance</u>	<u>Solids Flowrate to Thickener gm/min</u>	<u>So with Cataphoretic Assistance</u>
68.8	0.85	97.15	0.01
177.1	2.10	223.08	0.55
320.1	3.66	406.67	2.45

*The equation used to recalculate water density for transformations was:

$$(H_2O) = -0.000236 T^{\circ}C + 1.002509$$

Figure #19

<u>Time (hr)</u>	<u>So</u>	<u>Time (hr)</u>	<u>So</u>
1.33	1.65	5.58	1.08
1.83	1.66	6.08	1.08
2.33	1.64	6.58	1.02
4.08	1.37	7.08	0.98
4.58	1.28	7.58	0.96
5.08	1.19	8.08	0.97

Test begins at 0.83 hrs. Power off at 8.17 hrs.
Power on at 2.58 hrs.

Figure #21

<u>Time (hr)</u>	<u>So</u>	<u>Time (hr)</u>	<u>So</u>
2.77	1.63	6.58	0.93
3.30	1.57	7.08	0.86
3.80	1.61	7.58	0.78
5.00	1.40	8.08	0.74
5.58	1.26	8.58	0.76
6.08	0.98		

Test begins 1.75 hrs. Test ends at 8.75 hrs.
Power on at 4.00 hrs.

B30111